More intense daily precipitation in CORDEX-SEA regional climate models than their forcing global climate models over Southeast Asia

Phuong-loan Nguyen, Margot Bador, Lisa V Alexander, Todd P Lane, Thanh Ngo-Duc

Received: 10 August 2021 | Revised: 27 February 2022 | Accepted: 22 March 2022

DOI: 10.1002/joc.7619

RESEARCH ARTICLE

International Journal of Climatology RMetS

More intense daily precipitation in CORDEX-SEA regional climate models than their forcing global climate models over Southeast Asia

Phuong-Loan Nguyen[1,2] | **Margot Bador**[1,2,3] | **Lisa V. Alexander**[1,2] | **Todd P. Lane**[4,5] | **Thanh Ngo-Duc**[6]

[1]Climate Change Research Centre, UNSW Sydney, Sydney, New South Wales, Australia

[2]ARC Centre of Excellence for Climate Extremes, UNSW Sydney, Sydney, New South Wales, Australia

[3]CECI, Université de Toulouse, CERFACS/CNRS, Toulouse, France

[4]School of Geography, Earth and Atmospheric Sciences, The University of Melbourne, Melbourne, Victoria, Australia

[5]ARC Centre of Excellence for Climate Extremes, The University of Melbourne, Melbourne, Victoria, Australia

[6]Department of Space and Applications, University of Science and Technology of Hanoi, Vietnam Academy of Science and Technology, Hanoi, Vietnam

Correspondence
Phuong-Loan Nguyen, Climate Change Research Centre, UNSW Sydney, Sydney, NSW, Australia.
Email: phuongloan.nguyen@student.unsw.edu.au

Funding information
Australian Research Council, Grant/Award Numbers: CE170100023, DP160103439, FT210100459; LOTUS International Joint Laboratory

Abstract

The ability of regional climate models (RCMs) to accurately simulate the current climate is increasingly important for impact assessments over Southeast Asia (SEA), identified as one of the world's most vulnerable regions to climate change. In this study, we evaluate the performance of a set of regional high-resolution simulations from the Coordinated Regional Climate Downscaling Experiment-SEA (CORDEX-SEA) in simulating rainfall over the region. Simulations of the 1982–2005 seasonal mean climatology of daily precipitation and precipitation distribution over land are compared to observations from different sources (i.e., in situ-based and satellite-based). We also evaluate to what extent the precipitation distribution in RCMs is closer to observations than their associated forcing global climate models (GCMs). Observational estimates of precipitation over SEA have large uncertainties, making the model evaluations complicated. Despite these difficulties, our results highlight that RCMs can reproduce some complexities in the spatial distribution of seasonal rainfall but generally have a larger wet bias than GCMs. This is particularly true for the extremes in which RCMs show a large overestimation of rainfall intensity. There are some precipitation quantiles and grid points in which RCMs show limited reductions in biases compared to observations, but there is no consistency across all simulations and RCMs are generally further away from observations than their forcing GCMs. We find that greater intensity in RCMs over CORDEX-SEA compared to their associated forcing GCMs is firstly associated with the increased supply of moisture from both local and large-scale sources. Second, a widespread increase in convective precipitation is found across the region in RCMs. Our findings suggest that a model's ability to simulate precipitation over the region relies more on the RCM setup itself (e.g., parameterization scheme), rather than its forcing GCM. This should be considered when assessing the reliability of RCM precipitation simulations for future projections.

KEYWORDS
convective parameterizations, CORDEX-SEA, regional climate models, simulated precipitation

1 | INTRODUCTION

As evidence of climate change and its impacts continue to emerge, Southeast Asia (SEA) has been found to be one of the world's most vulnerable regions to climate change because of its long coastlines, heavy reliance on agriculture, and high dependence on natural resources and forestry (Weiss, 2009). The effects of climate change have potentially been exacerbated recently, leading to massive flooding, landslides and drought in many parts of the region (Hijioka *et al*., 2014; Chen *et al*., 2020; Tangang *et al*., 2020). Therefore, SEA, like other developing regions, needs to access robust information on the impacts of past and future climate change.

Most of SEA is located within the tropical climatic zone and its regional climate is strongly influenced by the Asian–Australian monsoon systems (Waliser and Gautier, 1993; Chang *et al*., 2005; Robertson *et al*., 2011). In addition to seasonal contrasts, the spatial distribution of precipitation is also heterogeneous due to complexities in its geographic distribution (e.g., 39% of the land is mountainous and there are many islands of varying size, Figure S1). Maximum precipitation in Indochina occurs during the boreal summer due to the monsoon from the Indian Ocean (Waliser and Gautier, 1993; Robertson *et al*., 2011) while many islands over the Maritime Continent receive large amounts of rainfall from the South China Sea during boreal winter (Waliser and Gautier, 1993; Chang *et al*., 2005). These complexities make it a challenge to simulate the seasonality and distribution of precipitation over the region.

Climate models are essential tools for providing information on the evolution of past climate, its variability and interaction with various components of the Earth system. Both global climate model (GCM) and regional climate model (RCM) have advantages and disadvantages which have been detailed in many previous research studies (Denis *et al*., 2002; Diaconescu and Laprise, 2013; Prein *et al*., 2016; Prein *et al*., 2019). GCMs have a comprehensive representation of the different Earth system components and are therefore generally used to explore climate interactions and underpin climate change projections through initiatives like the Coupled Model Intercomparison Project (CMIP; IPCC, 2013). However, they typically have a horizontal resolution of between 100 and 300 km, which limits their ability to account for important small-scale processes and the complex land surface heterogeneity of various regions, leading to large uncertainty in their simulations. These coarser GCMs can be replaced by the high-resolution RCMs (around tens of kilometres in the context of this study) over a defined region through one-way nesting approach (e.g., dynamical downscaling) by atmospheric variables and sea surface temperature obtained from GCMs. Numerous efforts and computational resources have been committed to developing RCMs, which produce simulations that try to better resolve the representation of complex surface characteristics (e.g., topography and land–sea contrast) (Torma *et al*., 2015) and small-scale atmospheric processes that are important drivers of regional climates (Giorgi and Bates, 1989; Di Luca *et al*., 2012).

Recently, the World Climate Research Programme's Coordinated Regional Climate Downscaling Experiment (CORDEX) initiative delivered downscaled simulations for various GCMs from CMIP Phase 5 (CMIP5; Meehl *et al*., 2000) to higher resolution regional models (Giorgi *et al*., 2008) for 14 regions worldwide. The decision on which GCMs to downscale can be subjective and depends on a particular region. Different horizontal grid spacings (i.e., 50, 44, 25 or 12 km) in RCMs have been also applied over different regions of the world with expected improvement compared to GCMs. This framework provides consistent high-resolution climate information for regional impact assessment. The evaluation of CORDEX RCMs and GCMs in simulating precipitation and the comparison of their respective performance have been performed in numerous studies for different parts of the world (e.g., Europe [Prein *et al*., 2016; Boé *et al*., 2020; Demory *et al*., 2020]; South America [Nikulin *et al*., 2012; Solman and Blázquez, 2019]; Australia [Di Virgilio *et al*., 2020]; East Asia [Lee *et al*., 2017; Park *et al*., 2019]). The main assumption investigated here and in most of the studies cited above is that RCMs should better simulate precipitation given their ability to capture processes at smaller scales than GCMs. These studies have been somewhat contradictory, sometimes showing improvements and sometimes not compared to their large-scale driving models (Diaconescu and Laprise, 2013; Giorgi and Gutowski, 2015). Though largely discussed, the extent to which high-resolution regional simulations outperform global simulations is still under debate and strongly depends on the scale, the variable under consideration, the region, and the metrics used. For example, CORDEX simulations over Europe (EURO-CORDEX)

and the Mediterranean (MED-CORDEX) show an improvement in the representation of mean climate compared to their driving GCMs over the complex topography Alpine region (Torma *et al.*, 2015; Giorgi and Gutowski, 2016). However, CORDEX-Africa exhibited significant biases for individual models over sub-regions, notably over arid and semiarid regions (Nikulin *et al.*, 2012). Another assumption is that any biases in RCMs are likely to be related to RCM configuration setup themselves when evaluating against the reanalysis-driven simulations (Kotlarski *et al.*, 2014) and/or they have inherited the systematic biases from their driving GCMs (Diaconescu and Laprise, 2013; Lee *et al.*, 2017).

Several evaluations of CORDEX simulations over SEA (CORDEX-SEA) have been performed, focusing on different aspects of precipitation over subregions like Thailand (seasonal mean precipitation, Tangang *et al.*, 2019), Malaysia (extreme precipitation, Tangang *et al.*, 2017) or the whole region (seasonal mean precipitation, Tangang *et al.*, 2020). In general, RCMs show reasonable agreement with observations but can have systematic wet biases due to a particular regional model (e.g., RegCM4). However, this type of model evaluation is often done such that the entire distribution of precipitation may not be evaluated. The improvement in an RCM simulation might simply be measured in terms of the degree to which one RCM simulation is closer to an observational reference than its paired GCM simulation from which boundary conditions were obtained. To date, limited studies over SEA assess whether RCMs represent an improvement over their driving GCMs in simulating rainfall patterns, except the recent work of Tangang *et al.* (2020) and Nguyen-Thi *et al.* (2021). Overall, Multi-Model Ensemble (MME) means of CORDEX-SEA RCMs displayed a better representation of climatological precipitation over areas of complex topography (Tangang *et al.*, 2020) but have a larger variability of rainfall compared to GCMs MME means (Nguyen-Thi *et al.*, 2021). However, the above studies focus only on the mean precipitation, based on a multi-model mean approach, and did not consider the performance of RCM–GCM pairs individually. Therefore, it is crucial to see whether the improvement of RCMs is observed in other aspects (i.e., the whole precipitation distribution) and consistently appears across all RCM–GCM combinations.

A challenge for evaluating the performance of a climate model relates to observational uncertainties. Indeed, many studies have highlighted large differences between different products of observations at the global (Donat *et al.*, 2016; Herold *et al.*, 2016, 2017; Alexander *et al.*, 2020; Bador *et al.*, 2020a) and regional (e.g., Europe [Kotlarski *et al.*, 2014; Prein *et al.*, 2016]; SEA [Nguyen *et al.*, 2020]) scales. At the global scale, observational uncertainties can be as large as inter-model spread (Herold *et al.*, 2016) while at regional scales the ranking of a particular model can be substantially changed by the observational reference data employed particularly for precipitation (Kotlarski *et al.*, 2019). Focusing on the Maritime Continent, Nguyen *et al.* (2020) found large inconsistencies in extreme precipitation intensity and inter-annual variability among various observational products due to a poor station network. Therefore, uncertainties related to the reference data should ideally be taken into account when assessing climate model performance in the present-day climate over SEA. Here we consider these inter-product differences in our model evaluation framework.

The objectives of this study are: (a) to evaluate an ensemble of CORDEX-SEA simulations with an ensemble of four observational datasets in order to assess the sensitivity of model performance to the choice of observational reference; (b) to determine differences between and identify the potential improvement of individual RCMs compared to their forcing GCMs in simulating the whole distribution of daily precipitation over both summer and winter seasons; (c) to further identify possible mechanisms for any identified differences between RCMs and GCMs.

The remainder of the paper is organized as follows. Section 2 describes the observational datasets and simulations used in this study along with the different metrics for model evaluation. Section 3 then outlines model performance, a comparison of the precipitation distributions between RCMs and GCMs, and the possible mechanisms behind identified differences, followed by a discussion and the conclusions in Sections 4 and 5, respectively.

2 | DATA AND METHODS

2.1 | Global and regional climate simulations

In this paper, we use the daily precipitation data from 11 CORDEX-SEA simulations running at 0.22° (about 25 km) horizontal grid spacing (Table 1). Following the modelling framework of the CORDEX project (Giorgi *et al.*, 2008), simulations from three RCMs are driven by boundary and initial conditions from the historical simulation of eight CMIP5 models. Only one simulation is available for each RCM–GCM combination. Further information on different physical schemes used in each RCM (i.e., convection parameterization, land surface and planetary boundary layer schemes) can be found in Table 1. To investigate the potential improvement of CORDEX simulations compared to their forcing GCMs,

TABLE 1 List of simulations from CORDEX-SEA analysed in this study

	RCM characteristics			GCM characteristics		Available information		
Simulation name	**Name**	**Convection scheme**	**Land surface scheme**	**Name**	**Resolution**	**Evaporation**	**Convective precipitation**	**References**
RCA4_CNRM-CM5	RCA4	Fritsch and Kain (1993)	Samuelsson *et al.* (2006)	CNRM-CM5	1.2° × 1.8°			Nikulin *et al.* (2012)
RCA4_HadGEM2-ES				HadGEM2-ES	1.25° × 1.875°	×	×	
REMO2015_MPI-ESM-LR	ROM	Tiedtke (1989)	Hagemann (2002) Rechid *et al.* (2009)	MPI-ESM-LR	1.8° × 1.8°	×	×	Sein *et al.* (2015)
REMO2015_HadGEM2-ES				HadGEM2-ES	1.25° × 1.875°	×	×	
REMO2015_NorESM1-M				NorESM1-M	1.9° × 2.5°	×	×	
RegCM4-3_CNRM-CM5	RegCM4	MIT-Emanuel (Emanuel and Rothman, 1999)	Biosphere-atmosphere Transfer Scheme (BAST1e) Dickinson *et al.* (1986)	CNRM-CM5	1.2° × 1.8°			Ngo-Duc *et al.* (2017) Juneng *et al.* (2016) Cruz *et al.* (2017)
RegCM4-3_CSIRO-MK-3-6-0				CSIRO-MK-3-6-0	1.865° × 1.875°			
RegCM4-3_EC-EARTH				EC-EARTH	1.125° × 1.125°	×	×	
RegCM4-3_GFDL-ESM2M				GFDL-ESM2M	2° × 2°	×	×	
RegCM4-3_HadGEM2-ES				HadGEM2-ES	1.25° × 1.875°			
RegCM4-3_MPI-ESM-MR				MPI-ESM-MR	1.8° × 1.8°	×	×	

we constrain our study to the subset of CMIP5 GCMs used for the CORDEX simulations (Table 1). The results of RCMs are evaluated to their driving GCMs. Note that an unweighted MME mean was also included for both RCM and GCM since it might reduce biases from individual model output and was widely used in previous studies (Ngo-Duc *et al*., 2017; Tangang *et al*., 2020).

The multi-model framework used in the present study presents two key features. First, for each of the three RCMs, an ensemble of simulations forced by different GCMs is available (two simulations for RCA4, six simulations for RegCM4-3, and three simulations for REMO2015; Table 1). This allows us to investigate potential commonalities explained by each RCM setup and potential differences due to the diversity in GCM boundary conditions imposed as forcing. Second, some simulations from different RCMs share similar GCM forcing conditions (i.e., RCA4, REMO2015 and RegCM4-3 forced by HadGEM2-ES, and RCA4 and RegCM4-3 forced by CNRM-CM5; Table 1). Given similar boundary conditions, differences across RCMs are likely related to their differences in physics, and in particular, the convective parameterization schemes, which have an important influence on precipitation. However, the drawback of our modelling framework is that all RCM simulations lack air–sea interactions and model nudging was not applied. Therefore, we cannot investigate the influences of methodological choices like spectral nudging and missing ocean-atmospheric coupling in RCMs, which might impact the RCM output (Colin *et al*., 2010; Yang *et al*., 2012).

2.2 | Observational datasets and domain

To address observational uncertainties, we utilize four gridded observational products of daily precipitation from different sources (i.e., three in situ and one satellite-based dataset). Three datasets of spatially interpolated in situ data are considered,: the Asian Precipitation-Highly Resolved Observational Data Integration Towards Evaluation of Water Resources (APHRODITE version V1101; Yatagai *et al*., 2012) a regional land-only product over Asia; two global land-based datasets that are the Rainfall Estimates on a Gridded Network (REGEN version Allstns V1 2019; Contractor *et al*., 2020) dataset, and the Global Precipitation Climatology Centre (GPCC version FDD_v2018; Schamm *et al*., 2014) dataset. We also consider remote sensed estimates of precipitation by using the Climate Hazards Group InfraRed Precipitation with Station (CHIRPS version 2.0; Funk *et al*., 2015) dataset, a quasi-global rainfall dataset that incorporates in situ climatology and satellite imagery.

These datasets have been selected because they have at least 24 years of data (over the period 1982–2005) and sufficient coverage over the Southeast Asian domain (90°–145°E; 15°–25°N, Figure S1). We do not consider those satellite products that do not account for a correction to rain gauges because these type of products are too inconsistent in climatology and trends in daily precipitation maxima over this region (Nguyen *et al*., 2020). Further information on the observational datasets is listed in Table 2. Note that we did not select the newest version of APHRODITE (i.e., V1901) due to its shorter time period (1998–2005) compared to its predecessor (i.e., V1101; 1951–2007) utilized here. In addition, Nguyen *et al*. (2020) also noted the limited difference between APHRODITE V1901 and V1101 in the representation of extremes, which gives further confidence in using the V1101 version here.

2.3 | Precipitation indices and evaluation metrics

In this research, the RCMs performance is evaluated over the climatological period 1982–2005, as this is the longest period common to all observational datasets and simulations.

RCM simulations are evaluated based on two aspects of precipitation: the mean state and daily precipitation distribution. The performance of a simulation in reproducing the observed climatology of seasonal daily mean precipitation is evaluated using different statistics including the spatial average (M), the root mean squared error (RMSE), and the spatial correlation (R). While M and RMSE measure the similarity between models and observations in terms of intensity, R provides information on the spatial distribution. Simulated and observed seasonal distributions of daily precipitation are compared by using quantile–quantile (Q–Q) plots (Figure S2). This simple metric offers insight into all quantiles of the distribution by mapping each quantile in one distribution with each quantile in another. To further measure how close or distant the simulated data is to the observed distribution, we develop an area score metric (ASM), which measures the area between the two lines (e.g., the red and black lines respectively, Figure S2) using the trapezium rule. Finally, we rank model performance based on RMSE and ASM to evaluate models individually and compare simulations across each other. The metrics mentioned above are also applied to examine the differences between RCMs and their forcing GCMs.

In order to measure the performance of each RCM and compare RCMs to observations, all daily observed and simulated precipitation fields are interpolated into a common grid of $1^\circ \times 1^\circ$ resolution using conservative remapping. For the spatial average over land, we used the common mask from REGEN_ALL.

TABLE 2 List of observational datasets of daily precipitation used in this study

Product short name	Product version	Temporal coverage	Original resolution	Type of data	References
APHRODITE	APHRODITE V1101	1950–2005	0.5° × 0.5°	In situ-based	Yatagai *et al.* (2012)
REGEN_ALL	REGEN Allstns V1 2019	1981–2019	1° × 1°	In situ-based	Contractor *et al.* (2020)
GPCC_v2018	GPCC FDD v2018	1982–2019	1° × 1°	In situ-based	Schamm *et al.* (2014)
CHIRPSv2	CHIRPSv2	1981–2016	0.05° × 0.05°	Satellite with correction to rain gauge	Funk *et al.* (2015)

To make a fair comparison between RCM and GCMs simulation, all observations and RCM simulations are interpolated into the coarsest forcing GCM grid (i.e., NorESM1-M, ∼240 km) (Table 1). Note that for the spatial average over the land, only grid points with a fraction of land greater than 0.5 are interpolated. The mask was extracted from the land–sea mask of NorESM1-M.

We further explore the differences between simulated and observed precipitation by analysing the moisture budget over the region of interest. Previous studies have suggested that regional precipitation is approximately balanced by local evaporation and remote moisture transportation on a mean seasonal time scale (Brubaker *et al.*, 1993; Li *et al.*, 2013; Demory *et al.*, 2014; Vannière *et al.*, 2019; Goergen and Kollet, 2021). We therefore express the moisture budget equation as:

$$\overline{P}-\overline{E}=\frac{1}{g}\overline{\nabla.\int_{p_t}^{p_s} q\,\vec{V}\,dp}.$$

where P is mean precipitation, E is evaporation, $\nabla.\int_{p_t}^{p_s} q\vec{V}dp$ is the vertically integrated moisture flux transported into and out of the atmospheric single column; q is specific humidity and $\vec{V}$ is horizontal wind. Due to CORDEX-SEA data availability constraints, we cannot calculate the vertically integrated moisture fluxes over the region. Therefore, we make the assumption that $P - E$-averaged over land should be equal to moisture convergence over land according to Li *et al.* (2013), Goergen and Kollet (2021).

3 | RESULTS

3.1 | Observed precipitation and its associated uncertainties

We first characterize the spatial distribution of seasonal mean observed daily precipitation and its associated uncertainties (Figure 1) during the 1982–2005 period. We consider four observational datasets (as mentioned in Section 2.2) and compare these distributions across the different products We find clear seasonal and regional contrasts in the precipitation pattern over SEA with generally high rainfall observed over Indochina during summer (June–July–August–September; JJAS) and less precipitation found in equatorial regions. On the contrary, Indochina receives less precipitation while the Maritime Continent receives more precipitation during the boreal winter (December–January–February; DJF). This "north-to-south dry-to-wet" gradient is mainly due to the influence of the Asian–Australian monsoon (Chang *et al.*, 2005; Robertson *et al.*, 2011; Juneng *et al.*, 2016; Tangang *et al.*, 2020). The southwest monsoon from the Indian Ocean is typically from late May to September and particularly affects Thailand and Myanmar, resulting in the rainy season there during JJAS. Meanwhile, the northeast monsoon, typically from November to March brings rainfall in the southern part of SEA in DJF and is associated with relatively dry and cool air and little precipitation to the mainland (Kamworapan and Surussavadee, 2019).

Overall, the spatial contrasts and the seasonal shifts of intense rainfall regions are quite similar among the four datasets considered but substantial differences are found in the intensity of climatological precipitation, notably during DJF. APHRODITE has a drier climatology compared with other products, whereas the other three datasets (i.e., REGEN_ALL, GPCC_v2018 and CHIRPSv2) show similar spatial pattern and intensity over the whole region. The differences across the four observational products are larger during summer compared to winter as shown by the regional averages (from 5.25 to 7.14 mm·day^{-1} compared to 4.01 to 5.80 mm·day^{-1}, respectively). Larger inter-product differences are found over sub-regions, up to 4 mm·day^{-1} relative to the climatology of APHRODITE in the equatorial regions during boreal winter (DJF).

Despite the broad similarity in the spatial distribution of daily mean precipitation, large discrepancies are found

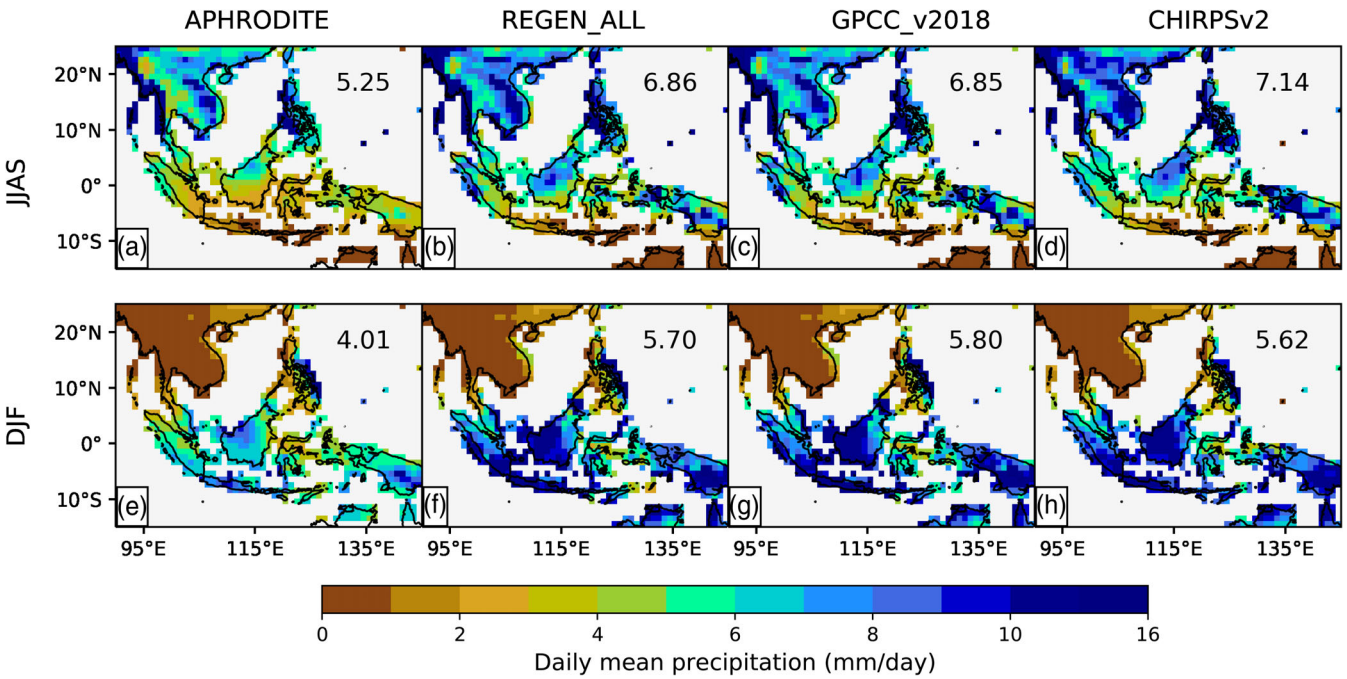

FIGURE 1 Seasonal mean (the boreal summer—JJAS and winter—DJF; row) of daily observed precipitation (mm·day^{-1}) from four considered observational products: APHRODITE, REGEN_ALL, GPCC_v2018 and CHIRPSv2 (column) during the climatological period of 1982–2005. ALL datasets are considered at a grid of 1° × 1° degree of resolution

in the different quantiles of the daily precipitation distribution. To illustrate this point, Q–Q plots (Figure S3) are used and quantiles of daily regionally-averaged precipitation distribution from various observational products are compared to the corresponding quantiles of the multi-product mean, highlighting the inter-product differences. Generally, from a quantile of 3 mm (i.e., in the first half of the distribution), APHRODITE consistently shows the lowest estimates of precipitation whereas GPCC_v2018 presents the highest estimates among all considered observational datasets. In addition, the quantiles of CHIRPSv2 and REGEN_ALL are quite similar to each other up to the value of the 50th percentile in both seasons. Subsequently, the quantiles related to higher precipitation amounts from all datasets increasingly diverge from each other, with maximum variance observed in the highest quantiles (greater than the 99th percentile).

This inter-comparison of seasonal climatologies in daily precipitation is in line with the previous regional studies on mean (Juneng *et al.*, 2016; Tangang *et al.*, 2020) or extreme precipitation (Nguyen *et al.*, 2020), highlighting the substantial uncertainties among different observations over the region.

3.2 | Model performance

We then compare seasonal means of daily precipitation in the RCM simulations (over the 1982–2005 period) with the different observational reference products used in this study. We focus primarily on the differences in the spatial distribution of daily precipitation between RCM simulations and APHRODITE (Figures 2 and 3). Indeed, despite the large observational uncertainties over the regions mentioned in Section 3.1, the maps of differences between RCM simulations and the different observational products show a similar pattern (Figure S4). Therefore, we take the map of the differences between the ensemble mean of RCMs (ENS-RCM, Figures 2a and 3a) and all 11 simulations (Figures 2b–l and 3b–l) relative to APHRODITE to illustrate the following common observed features. We first discuss the key features of summer season (JJAS; Figure 2). Models reveal good qualitative correspondence with the gross regional distribution. The spatial correlations between the simulated and observed patterns are around 0.5 for most models (8 out of 12). Second, most models generally show a wetter bias in terms of regional-average but exhibit an inhomogeneous spatial distribution with mixing of dry and wet biases. Interestingly, the spread of the climate model ensemble (i.e., summer biases relative to APHRODITE ranging from 0.53 to 5.68 mm·day^{-1}, Figure 2) is greater than the spread of reference datasets (ranging from 5.25 to 7.14 mm·day^{-1}, Figure 1a–d).

The corresponding results for boreal winter (Figure 3) reveal some interesting features. First, all models can reproduce the summer to winter shift in precipitation from Indochina to the Maritime Continent. This shift reflects the 'north-to-south dry-to-wet' gradient which is

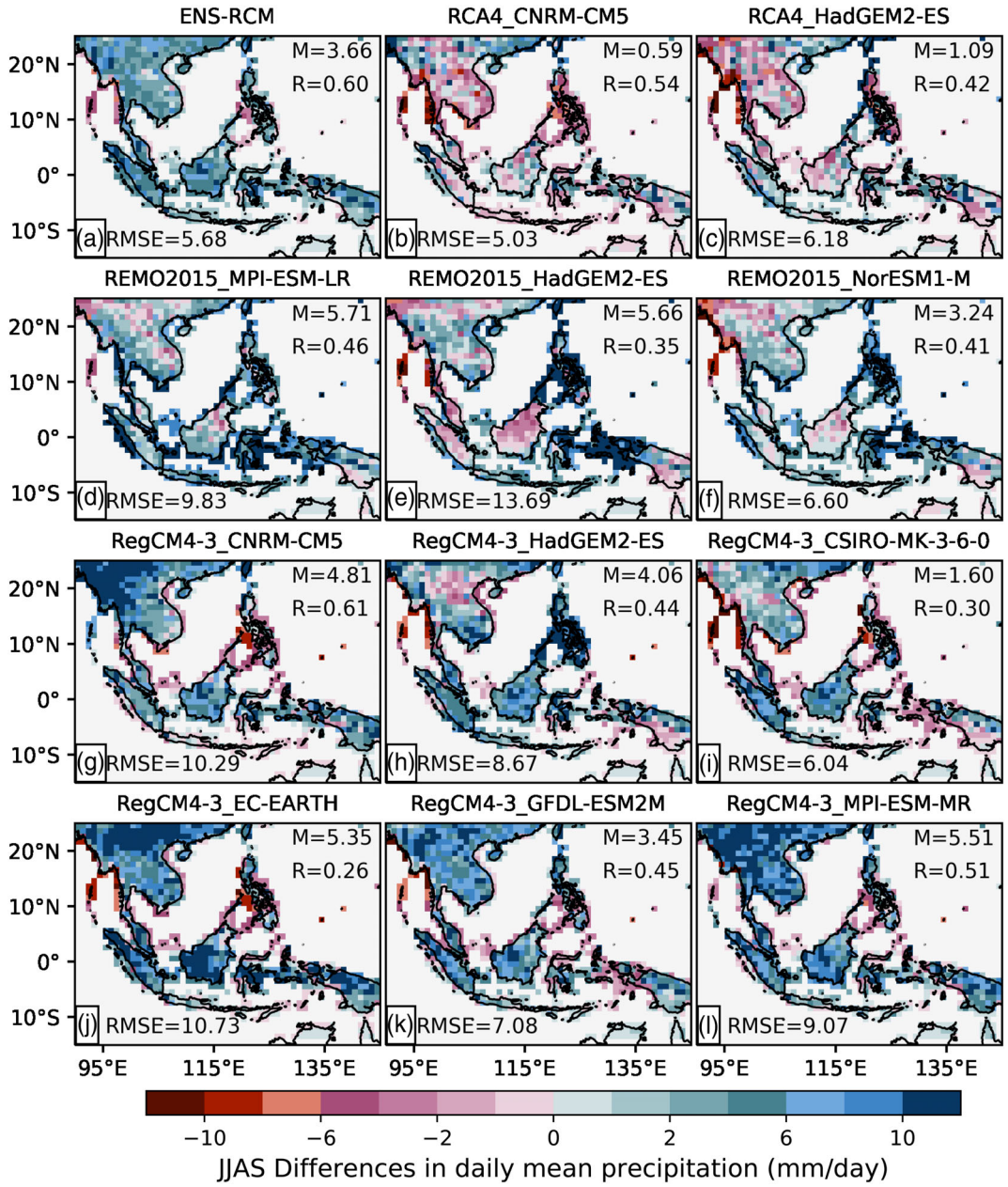

FIGURE 2 Differences (in mm·day^{-1}) in seasonal mean of daily precipitation between all RCMs simulations and APHRODITE. All simulations are interpolated onto a 1° × 1° degree grid. Inserted numbers indicate: The difference in regional mean (M), the root mean square error (RMSE) and the spatial correlation of climatological seasonal mean of daily precipitation in RCMs with APHRODITE (R)

discernible in observed precipitation (Section 3.1). Third, better spatial correlation between simulations and observations are found during winter, highlighting the dependence of model performance on season. In addition, the wetter biases are domain-wide, and they have smaller magnitude than in summer. Finally, it is interesting that the less prominent inter-model differences are found in the spatial distribution of winter daily precipitation intensity compared with that in summer. In particular, all models show consistently smaller biases over Indochina and larger biases over Maritime Continent.

Taking into account different reference products, there are some interesting features that emerge (Figure S4). Biases in simulations relative to REGEN_ALL, GPCC_v2018 and CHIRPSv2 are quite similar but show some differences to those biases relative to APHRODITE. For instance, the RegCM4-3_CSIRO-MK-3-6-0 combination is quite close to REGEN_ALL, GPCC_v2018 and CHIRPSv2 (biases of −0.14, −0.12 andc−0.27 mm·day^{-1}, respectively) but farther from APHRODITE (bias of 1.60 mm·day^{-1}, Figure 2i) during the boreal summer, highlighting the difficulties in model evaluation due to large observational uncertainties over

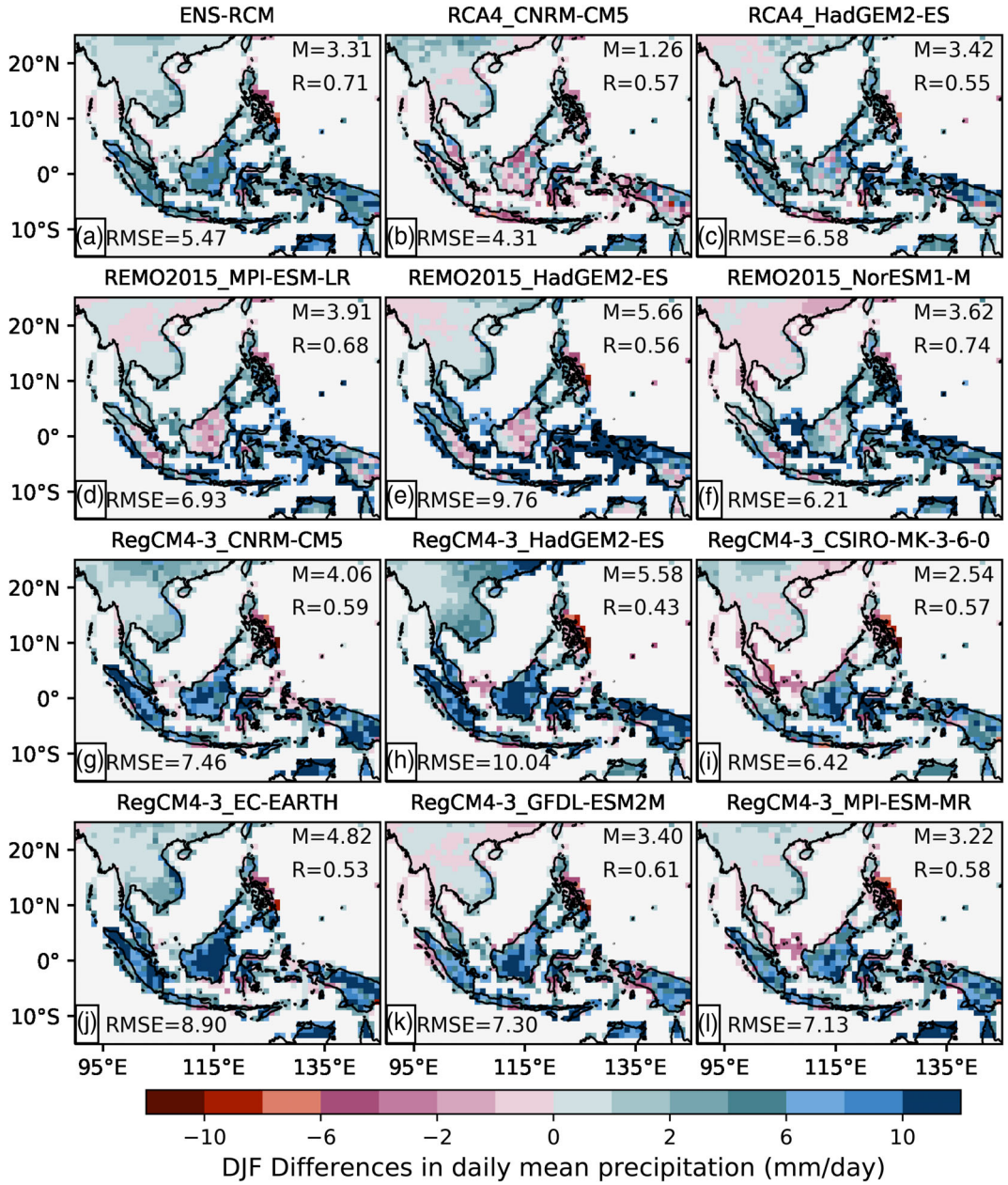

FIGURE 3 Same as Figure 2 but for the boreal winter (DJF)

SEA. This agrees with previous studies showing how discrepancies among observations make model evaluation difficult at the global scale (Bador *et al.*, 2020b).

Despite large observational uncertainties, some robust conclusions still emerge from the analysis. First, most simulations (notably simulations from RegCM4-3) produced consistently wet biases, no matter the choice of observational product. There are some exceptions with some simulations from RCA4 and REMO2015 exhibiting different signs of biases, depending on the choice of reference. Second, models are able to simulate the complexities in spatial distribution of precipitation over the region in both seasons (spatial correlations around 0.5). Third, the multi-model means show a consistently better performance (lower RMSE, higher spatial correlation with observations) than each individual RCM's simulation.

To gain an overview of the performance of each model, we ranked 11 simulations and multi-model mean (RCM-ENS) against the four observational products during different seasons using RMSE (with 1 being the best performing and 12 the worst-performing RCM–GCM combinations; Figure 4). RMSE is calculated for the climatology of seasonal mean precipitation (over the 1982–2005 period) and allows further evaluation of model agreement with observations by measuring the similarity in terms of intensity of mean daily precipitation. First, we

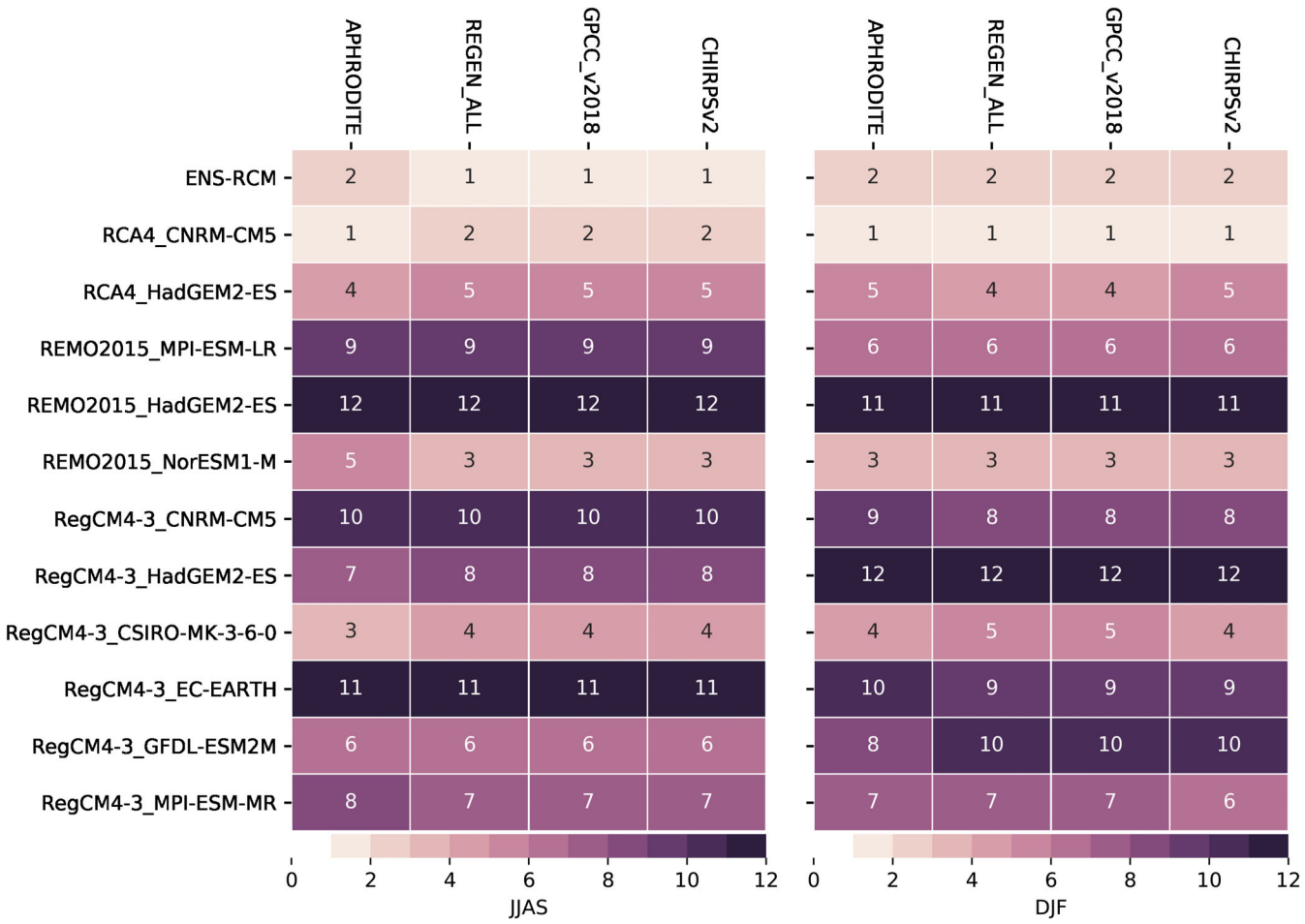

FIGURE 4 Ranking of RCM simulations (Table 1) based on the root mean square error (RMSE) with 1 indicating the best model performance and 12 indicating the worst model performance. The RMSE is estimated based on the difference between historical RCM simulations and observations during the climatological period of 1982–2005

note that simulations are similarly ranked (i.e., with few exceptions) in both seasons when using different observational references, emphasizing their similarity in terms of intensity and precipitation distribution. REGEN_ALL and GPCC_v2018 shared the exact same ranking across models as this could be expected from their common data structure (building upon the same station network—see Roca *et al*., 2019). Second, some models indicate a consistent performance during both seasons, being always better (i.e., ENS-RCM, RCA4_CNRM-CM5 and REMO2015_NorESM1-M) or always worse (i.e., REMO2015_HadGEM2-ES and RegCM4-3_EC-EARTH) than others.

3.3 | Comparison of daily precipitation between RCMs and their forcing GCMs

A major objective of this study is to assess whether the RCMs improve the representation of daily precipitation over the region compared to their forcing GCMs. To that end, we use Q–Q plots and compare ASM (Section 2.3) for each RCM–GCM combination. Note that the quantiles of model ensembles are calculated by pooling the values from all models.

We first consider the ranking of ASM applied to daily regionally-averaged precipitation (Figure 5) and find some discrepancies between RMSE ranking and ASM ranking (Figure 5 vs. Figure 4). Unlike RMSE, the ASM ranking is sensitive to the choice of reference product used for model evaluation, notably for RCA4 and REMO2015 simulations. For example, a difference in the ranking of RCA4_CNRM-CM5 is found during both seasons and is as large as five places depending on the reference product. This demonstrates again how large observational uncertainties can be when taking different precipitation percentiles into account (see also Figure S3).

The model simulation changes rank depending on the metric considered. Notably, the distribution of mean precipitation in RegCM4-3_GFDL-ESM2M is in the

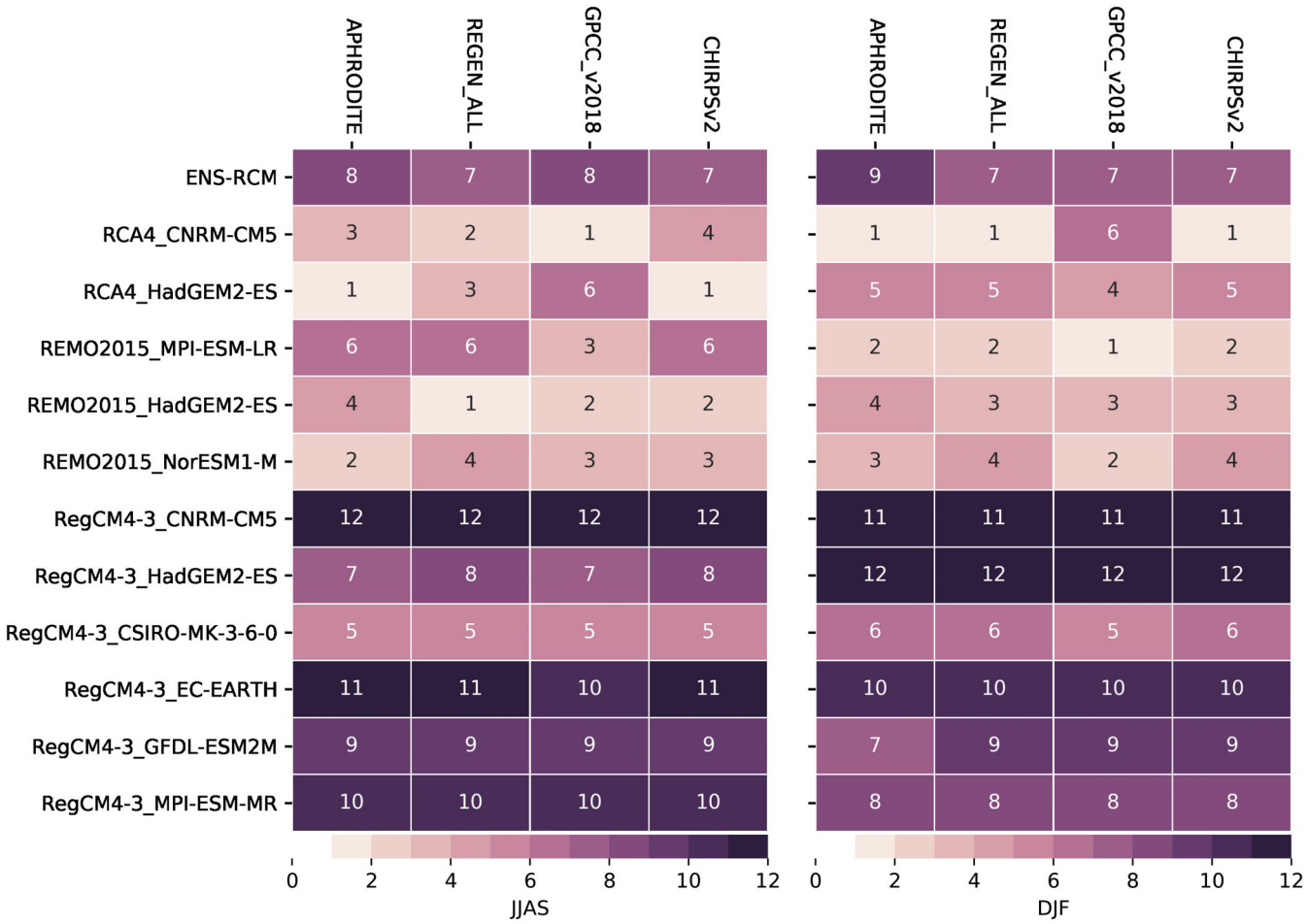

FIGURE 5 Ranking of RCM simulations (Table 1) based on the area score metric (ASM) which measure the proximity between the two distributions: RCMs and observational precipitation distribution. Number 1 indicates the best model performance and Number 12 indicates the worst model performance

middle of the model range (ranked 6 during summer based on RMSE) but shows less skill when the full precipitation distribution is considered (ranked 9 based on area score). This lower performance for ASM is mainly due to higher precipitation quantiles. This reveals the limitation of RCM simulations to estimate extreme events and might be attributed to the difference in frequency of rainfall between RCMs and observations (see more in Section 4). Interestingly, all RCA4 and REMO2015 simulations generally indicate better performance than RegCM4-3, no matter the choice of observational reference or skill metrics. Almost all RegCM4-3 simulations except RegCM4-3_CSIRO-MK-3-6-0 are consistently 'worse' compared to other simulations. Rankings of models based on ASM are generally similar when using APHRODITE, REGEN_ALL and CHIRPSv2 as reference but exhibit significant changes when using GPCC_v2018 as reference. Therefore, we hereafter take only APHRODITE and GPCC_v2018 to illustrate the substantial impact of observational uncertainty on model performance.

Simulated daily regionally-averaged precipitation quantiles in both RCMs and GCMs over the terrestrial RCM domain are plotted against the quantiles of APHRODITE and GPCC_V2018 over the climatological period of 1982–2005 (Figures 6 and 7 for the boreal summer and winter, respectively). There is often a clear shift to higher estimates of precipitation in RCMs compared to their forcing GCMs. In most cases, the RCM simulations (red) are above their forcing GCMs (blue), indicating more intense precipitation in RCMs and generally a wet bias as the red line usually sits above the observations. Most GCM distributions also sit above the observations indicating, often but not always, a wet bias. We note though that some GCM simulations (e.g., EC-EARTH (j), HadGEM2-ES (c, e, h) and MPI-ESM-LR or MR (d, l); Figures 6 and 7) are similar to APHRODITE (i.e., they lie on or near to the black 1:1 line). In addition, differences between RCM and GCM distributions are usually amplified for the highest percentiles. These interesting features are also observed when we pool the results from all

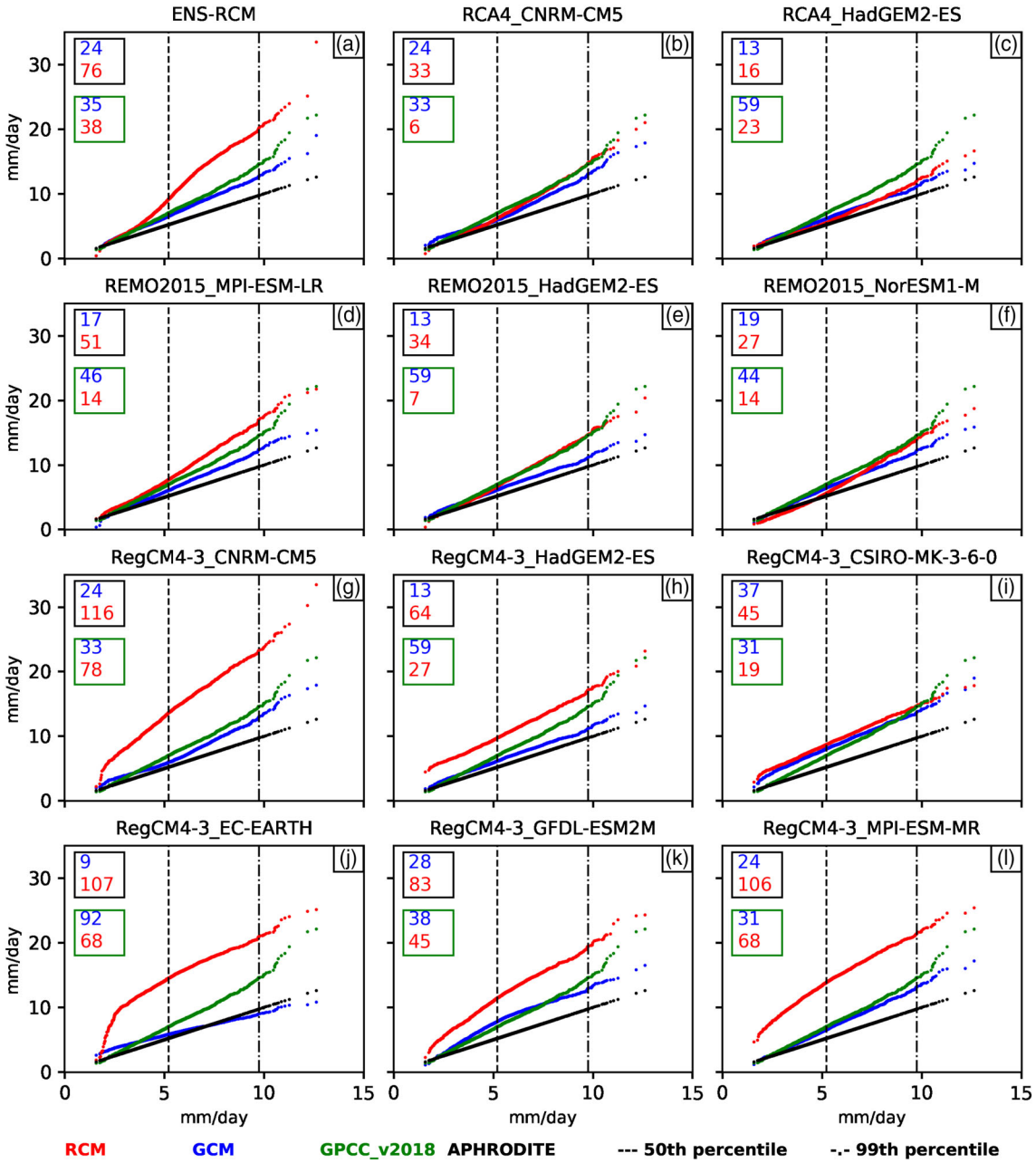

FIGURE 6 Quantile–quantile plots for daily regionally-averaged precipitation (in mm·day^{-1}) during the climatological period of 1982–2005 from different RCMs (red), their forcing GCMs (blue), and the GPCC_v2018 observational product (green) against APHRODITE (black) for the boreal summer (JJAS). All simulations are on the coarsest forcing GCM grid (i.e., NorESM1-M, ~240 km). Inserted numbers (within black and green box) indicate values of the area score metric (ASM) which measure the proximity between the two distributions

simulations and consider them as the model ensemble mean (ENS-RCM, Figures 6a and 7a), or average each quantile in the precipitation distribution across all simulations to calculate the quantiles for the ensemble mean (Figure S7).

The differences in ASM between an RCM and its forcing GCM can be very sensitive to the choice of observational dataset. In particular, when taking APHRODITE (or REGEN_ALL, CHIRPSv2; see Figures S5 and S6) as a reference, RCM area scores are mostly larger (i.e., RCM simulations are further away from observations) than that of their forcing GCMs. However, the reversed relative relationships between RCMs and GCMs are observed among 8 out of 11 pair simulations during both seasons (including RCA4, REMO2015 and some RegCM4-3 simulation, Figures 5 and 6) when taking GPCC_v2018 as a reference. It is interesting that the position of ENS-RCM and ENS-GCM lines are also changed with respect to

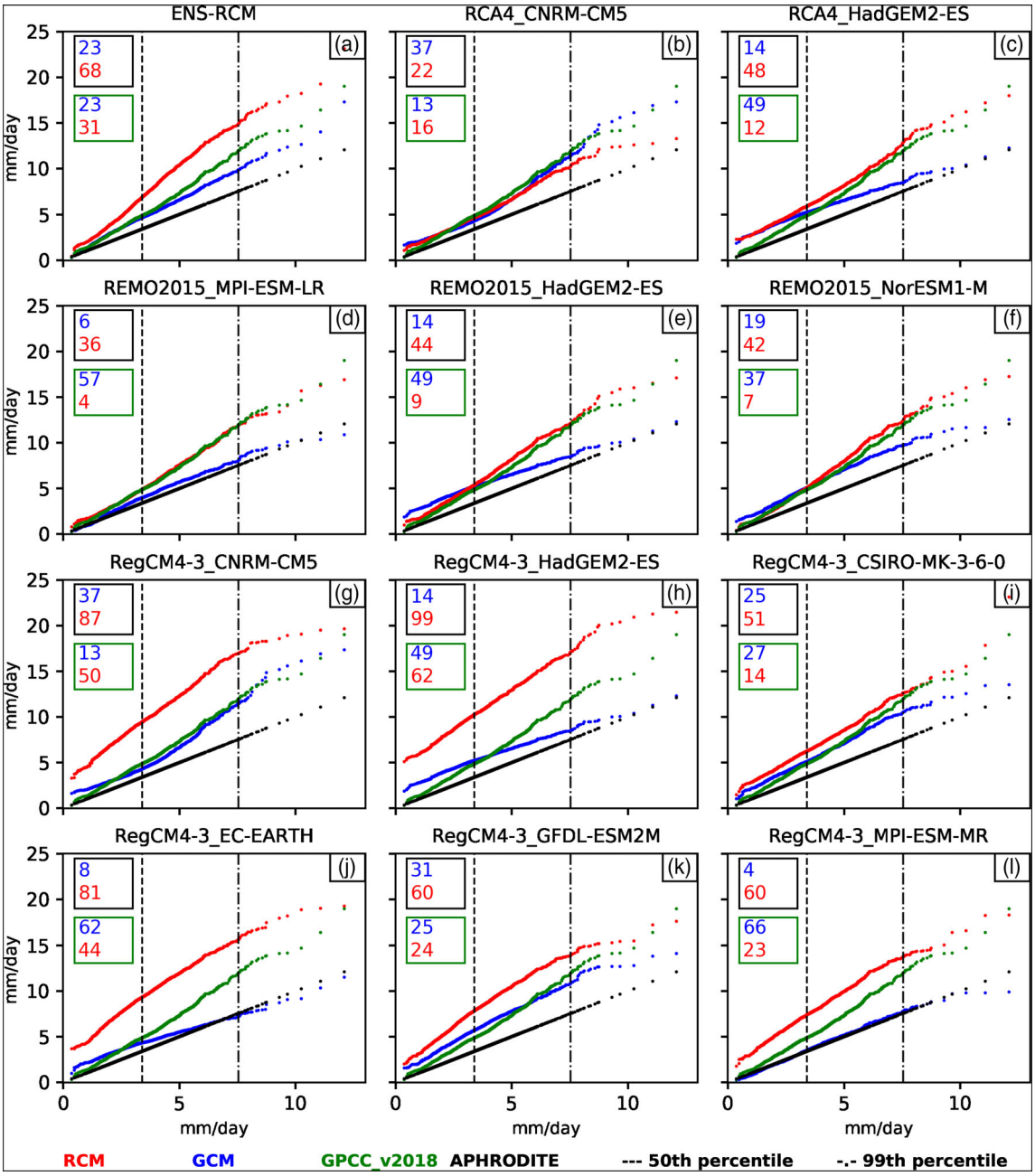

FIGURE 7 Same as Figure 6 but for the boreal winter (DJF)

different observational products with ENS-RCM being closer to GPCC_v2018 than ENS-GCM. This feature is consistent with the findings from Tangang *et al.* (2020), who indicated that the MME mean of RCMs show potential improvement compared to the MME mean of their forcing GCMs. The sensitivity of ASM to various observational products is consistent with large discrepancies in different precipitation percentiles among the various references mentioned in Section 1, notably at the highest percentiles.

Note that there are some parts of precipitation distribution in some cases (e.g., RCA4 and REMO2015 simulations) for which the RCM shows improvement compared to its driving GCM. To illustrate this point, three precipitation intervals are considered, including: 0–50th percentile (before the dashed line), 50–99th percentile (between the dashed and dot-dashed line), and greater than 99th percentile (after dot-dashed line) (Figures 6a and 7). For the lowest two percentile ranges, the RCA4 and REMO2015 simulations have very similar distributions to their forcing GCMs. Interestingly, in this driest part of the distribution, RCMs are sometimes closer to the observed reference datasets than the GCMs. This interesting feature can be observed

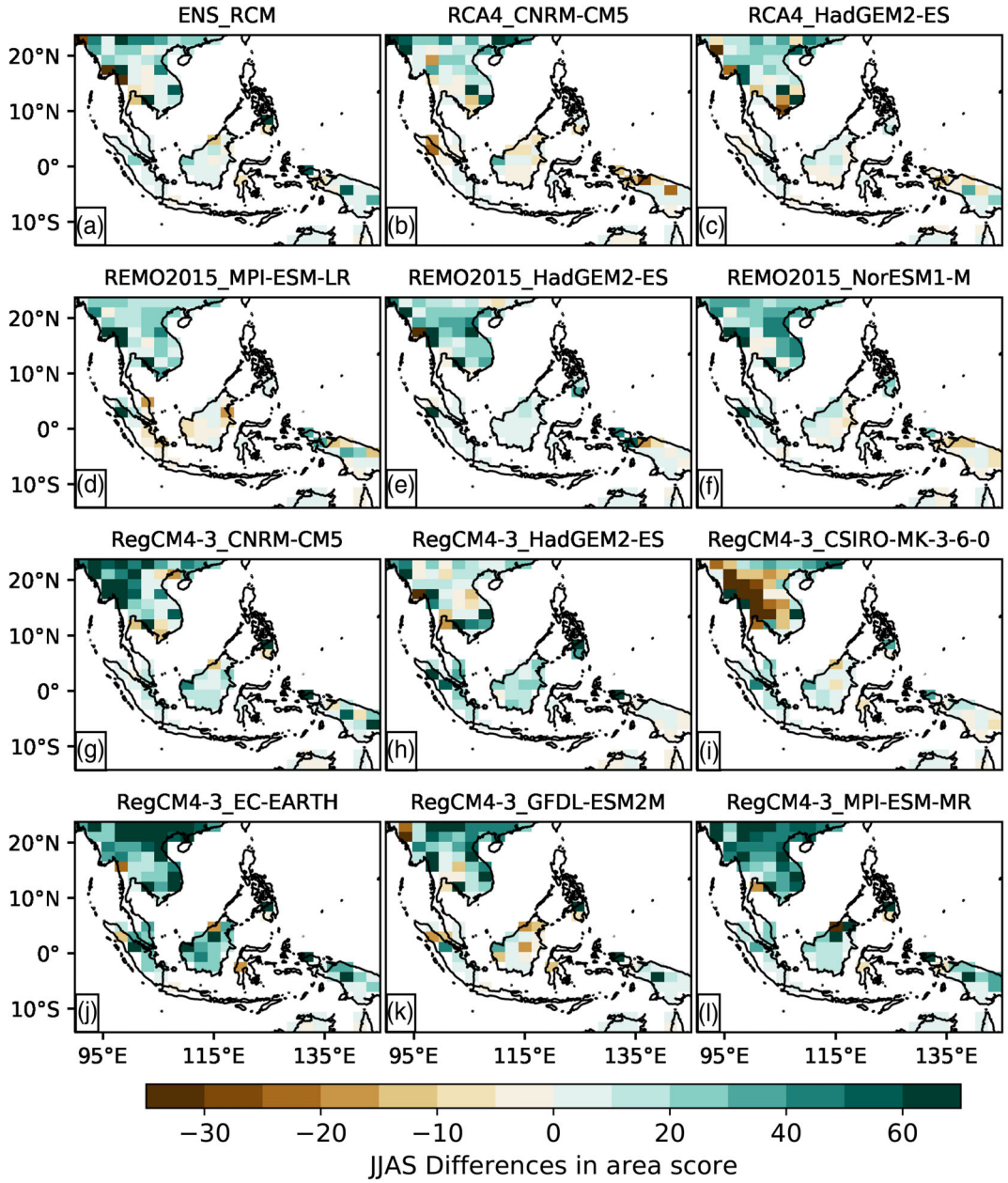

FIGURE 8 Differences in spatial distribution of area score metric (ASM) between RCMs and their forcing GCMs during the boreal summer (JJAS). The ASM values measure the proximity between two distributions: The RCM or forcing GCM simulations and APHRODITE precipitation distribution. All simulations are on the coarsest forcing GCM grid (i.e., NorESM1-M, ~240 km)

in most RCA4 and REMO2015 simulations during both seasons, except REMO2015_MPI-ESM-LR. However, at the highest percentiles (greater than 99th percentile), the RCMs are very different from their forcing GCMs and reference datasets, highlighting difficulties with these RCMs in estimating precipitation extremes. Meanwhile, RegCM4 simulations stand out as being much wetter and having distributions further from observed distributions than their forcing GCMs across all precipitation percentiles.

We further analyse how much improvement (or not) RCMs bring to the representation of daily precipitation distributions compared to their forcing GCMs by analysing the spatial distribution of differences in ASM using APHRODITE as a reference (Figures 8 and 9 for summer and winter, respectively). During the boreal summer, we find positive differences in ASM (blue colours) over most regions across all GCM-driven RCM simulations (Figure 8). This indicates the RCMs are further away from observed precipitation distributions than their

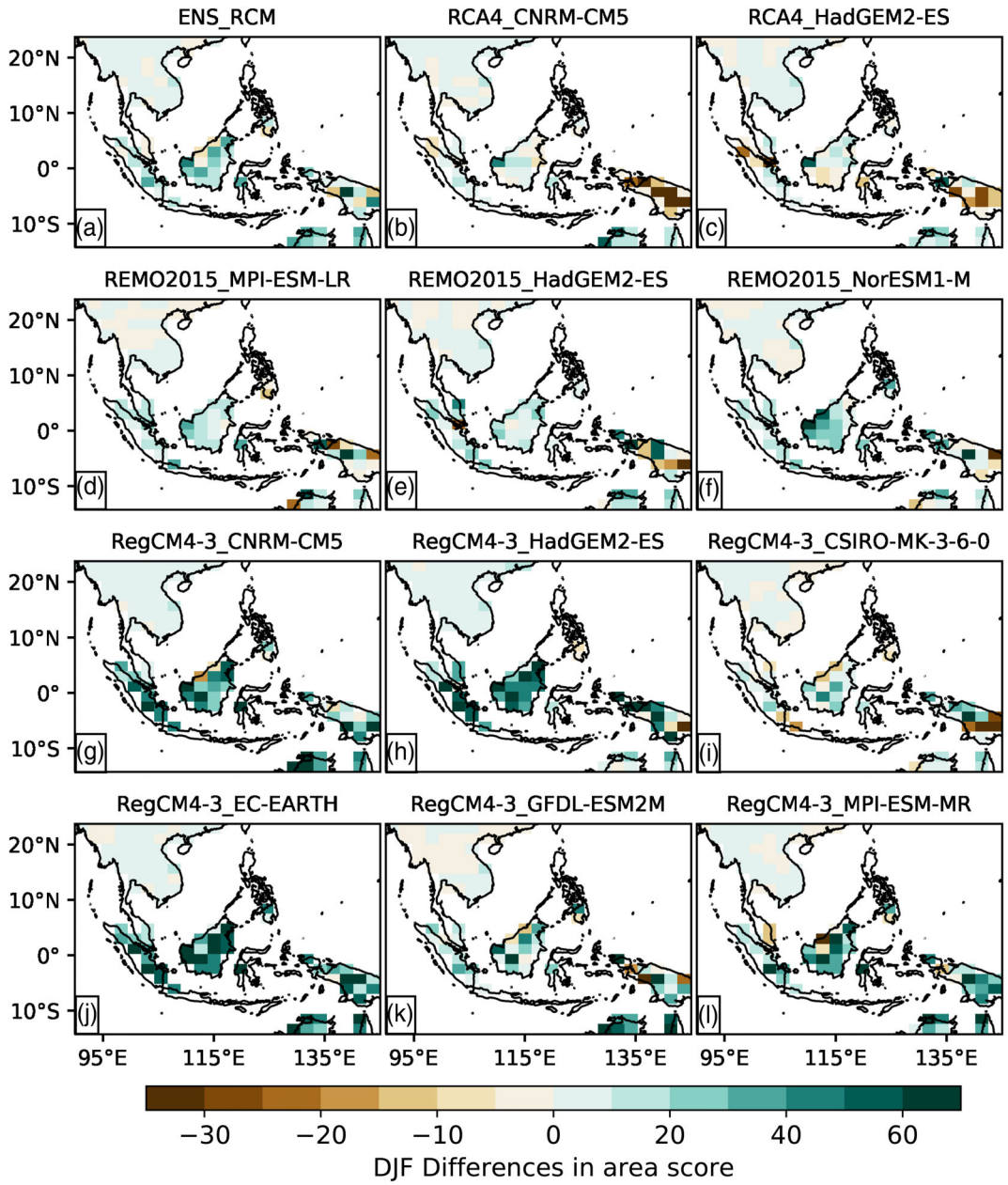

FIGURE 9 Same as Figure 8 but for the boreal winter (DJF)

forcing GCMs, over most parts of the region. The pattern during the boreal winter indicates fewer differences with little or no differences between RCM and GCM skill in estimating the whole distribution of precipitation over Indochina in most paired simulations. However, there are significant positive differences observed over many islands of the Maritime Continent (Figure 9). We also find some grid points associated with improvement in simulating daily precipitation (brown colours) in both seasons (Figures 8i and 9c). However, these areas are usually smaller in size and magnitude than regions of intensification. In addition, there is no agreement across all simulations on these regions during both seasons. In general, all combinations show consistently worse scores for RCMs than GCMs. Interestingly, the maps of area score differences are quite consistent with the differences in daily mean precipitation in both seasons (spatial correlations are greater than 0.5 in most cases for both seasons as illustrated in Table 3). This implies that the mean biases (as well as the ASM relative to different reference datasets, see more in Figure S8) are worse in RCMs and that the whole precipitation distribution in the RCMs analysed is further away from observations.

It is essential to explore whether the quality of RCM simulations relates to the internal skill of the RCM itself or the quality of its driving GCM. The relationship

TABLE 3 Spatial-averaged (M) and spatial correlation coefficient (R) of differences in the climatology of seasonal daily mean precipitation and in the area score metric (ASM) between RCMs and their forcing GCMs

		Summer (JJAS)		Winter (DJF)	
Model name	**Forcing GCM**	**Spatial-averaged differences (M, mm·day^{-1})**	**Spatial correlation coefficients (R)**	**Spatial-averaged differences (M, mm·day^{-1})**	**Spatial correlation coefficients (R)**
RCA4_CNRM-CM5	CNRM-CM5	−0.1	0.5	−0.5	0.8
RAC4_HadGEM2-ES	HadGEM2-ES	−0.8	0.4	0.3	0.8
REMO2015_MPI-ESM-LR	MPI-ESM-LR	1.6	0.6	1.4	0.9
REMO2015_HadGEM2-ES	HadGEM2-ES	0.2	0.5	0.3	0.8
REMO2015_NorESM1-M	NorESM1-M	−0.5	0.7	0.2	0.8
RegCM4-3_CNMR-CM5	CNRM-CM5	7.2	0.5	4.7	0.7
RegCM4-3_HadGEM2-ES	HadGEM2-ES	3.7	0.6	5	0.8
RegCM4-3_CSIRO-MK-3-6-0	CSIRO-MK-3-6-0	3.9	0.7	1.2	0.8
RegCM4-3_EC-EARTH	EC-EARTH	0.5	0.6	5.3	0.9
RegCM4-3_GFDL-ESM2M	GFDL-ESM2M	8.5	0.6	1.9	0.9
RegCM4-3_MPI-ESM-MR	MPI-ESM-MR	7.3	0.5	4.3	0.9

between regionally-averaged RCM and GCM biases and their nominal resolutions are further analysed in Figures 10 and 11. Most RCM–GCM combinations indicate more intense estimates of regionally-averaged means of precipitation in RCMs compared to their forcing GCMs (points above the 1:1 line in Figure 10). We cannot find a relationship between the regional averages of seasonal RCM biases and GCM biases in both seasons, which indicates that biases in the boundary conditions extracted from the GCM do not seem to have a direct impact on the driven RCM performance (Figure 10). Similarly, there is no relationship between the RCM biases and their forcing GCM's nominal resolution (Figure 11; note that the nominal spatial resolutions in GCMs are identified as a function of the total number of grid points over land). This indicates that forcing an RCM with a relatively high- or low-resolution grid GCM has limited influence on its representation of precipitation, and indeed RegCM4-3 forced by MPI-ESM-MR (the finest grid resolution in the ensemble) has among the worst biases across the simulations in boreal summer (Figure 11a).

3.4 | Exploring mechanisms behind the biased simulation of precipitation in RCMs

Given the somewhat larger wet biases that we have identified in RCM-simulated rainfall compared to the forcing GCM, we want to go one step further by exploring the mechanisms responsible for the origin of this extra moisture in RCMs. Therefore, the direct comparison of precipitation (P), evaporation (E) and moisture convergence ($P - E$) over land among and between seven RCM–GCM pairs (Table 1) are conducted in this section (Figure 12).

Figure 12 highlights the generally more intense regionally-averaged daily mean precipitation over land in most RCMs simulations compared to their forcing GCMs (5 out of 7 during the boreal summer and 7 out of 7 during the winter). RegCM4-3 especially is consistently wetter than other RCMs and their forcing GCMs. Further analyses on moisture sources indicate that both local and large-scale sources of precipitation contribute to these higher estimates of precipitation in RCMs. Moisture convergence is most likely the dominant contribution to these increases, notably during JJAS and in the RegCM4-3 simulations. During winter, contributions from the two sources are quite similar to each other and highlight the important role of local scale processes over tropical regions.

Orography triggers more precipitation in RCMs, and it is balanced by an increase in moisture convergence as mentioned in Tangang *et al.* (2020). This is confirmed by the fact that most regions associated with increases in precipitation (Figures 8 and 9) are on the windward side of high topography (Figure S1b). Therefore, we test

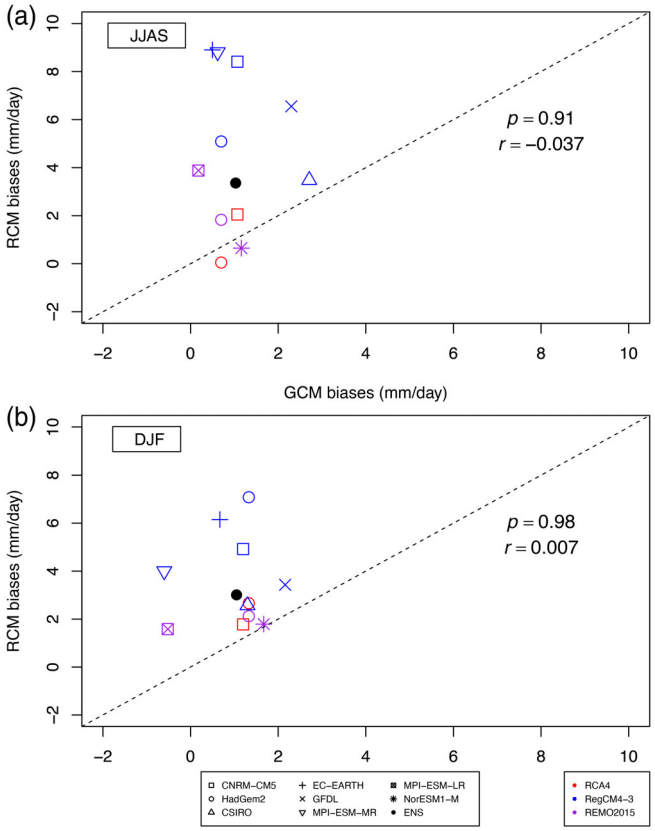

FIGURE 10 Scatter plots showing the relationship between the seasonal (JJAS and DJF) RCMs biases and their forcing GCMs biases (relative to APHRODITE). The dash line indicates the 1:1 line. The regression coefficients (r) and the p value are based on the F-test at a level of confidence of 5%

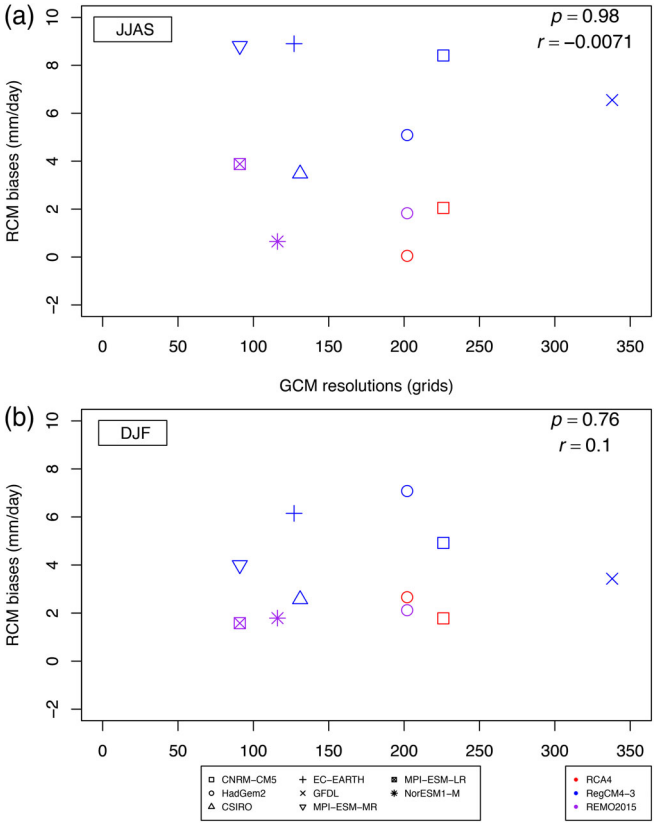

FIGURE 11 Scatter plots showing the relationship between the seasonal RCMs biases relative to APHRODITE and their forcing GCMs resolution. The solid line represents the regression line between RCMs and GCMs biases. The regression coefficients (r) are based on the F-test at a level of confidence of 5%

another hypothesis potentially explaining why the moisture convergence on land increases: that more moisture is transported from ocean to land.

Due to limitations in data availability, we cannot calculate vertically integrated moisture fluxes. Instead, we calculate the mean of horizontal wind, moisture convergence and specific humidity at 850 hPa for the four RCM–GCM combinations for which data are available. We acknowledge that due to the omission of vertical integration of the whole atmospheric level (Seager *et al.*, 2010; Seager and Henderson, 2013; Endo and Kitoh, 2014), precipitation and moisture convergence are not fully comparable at this single level. However, strong temporal correlations ($r > .6$, not shown) are found over some regions like South Indochina and western Borneo between differences in vertically integrated moisture fluxes ($P - E$) and differences in convergence fields at 850 hPa. This indicates that differences in moisture convergence at 850 hPa can be used as a good indicator of moisture convergence differences over these subregions. Our results show that moisture comes from different sources, depending on simulations (Figure S9). For example, there is increased wind and moisture convergence advected from ocean to land in RCA4_HadGEM2-ES. In particular, increasing wind from the South China Sea during boreal winter brings humid conditions (increased specific humidity) to South Indochina. Meanwhile, due to changes in the mean distribution of moisture over the Indian Ocean, Borneo also exhibits an increase in moisture convergence. This feature can be observed over REMO2015_MPI-ESM-LR during summer, where the intensification of wind from the Indian Ocean brings numerous amounts of moisture into South Indochina, resulting in stronger convergence and more humid conditions over there. However, the mechanism mentioned above is not clear across other simulations and cases. This indicates the limitation in our analysis and the question remains on where the additional moisture comes from.

The comparison between RCMs and their forcing GCMs raises the question of the contribution of

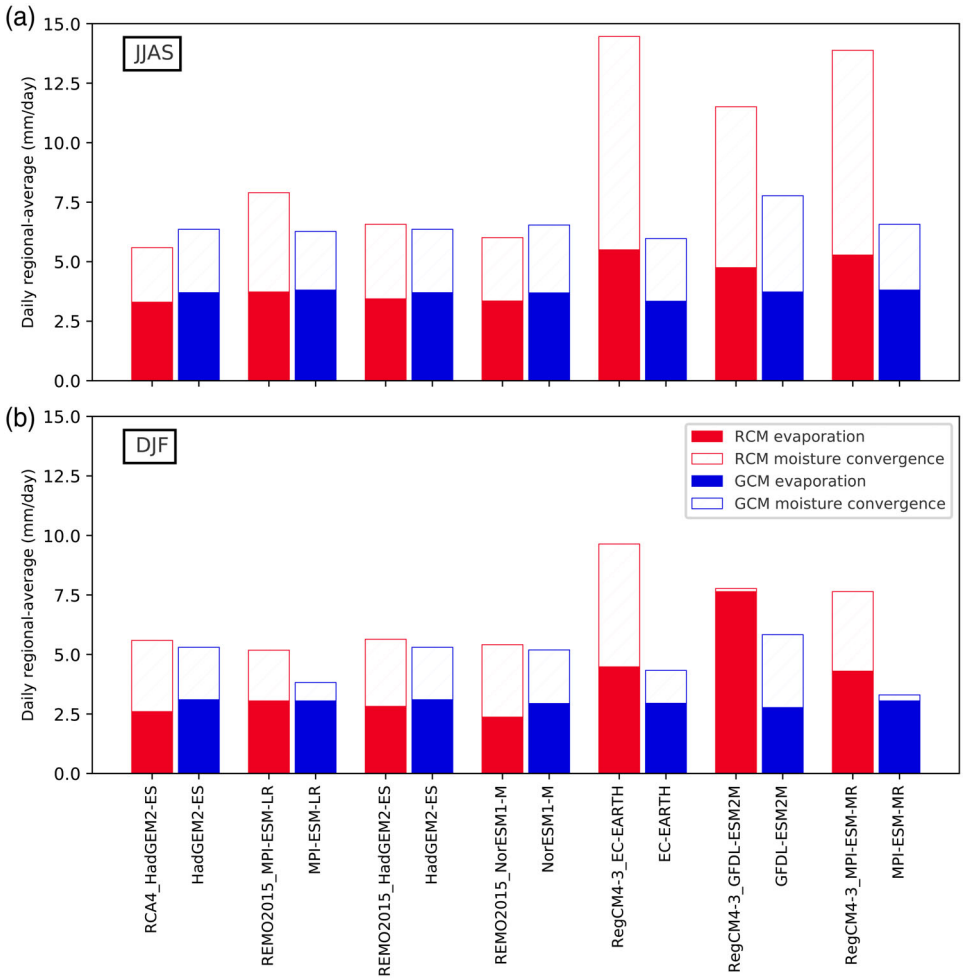

FIGURE 12 Seasonal (JJAS and DJF) mean of daily regionally-averaged evaporation (colour-filled) and moisture convergence (colour dashed) (land only; in mm/day) simulated by seven available RCMs simulations (Table 1) (red) and their associated forcing GCMs (blue) during the climatological period of 1982–2005

convective processes in each to daily total precipitation. Therefore, we further investigate whether precipitation differences presented in Table 3 correspond to differences in simulated convective and non-convective processes. Figure 13 compares regional averages of convective and stratiform precipitation simulated by the different RCMs and their forcing GCMs. First, the GCMs demonstrate that they typically simulate, and overestimate convective precipitation compared with MERRA2 (Figure S11). Convective precipitation also has largely contributed to the regional water budget at all RCM and GCM simulations. Second, we find a much greater increase in convective precipitation than non-convective term over land in RCMs, notably in the RegCM4-3 simulations during the boreal summer. Furthermore, the RegCM4-3 simulations stand-out throughout our whole analyses as having much wetter biases compared to their forcing GCMs, other RCMs and observations (more easily seen by comparing different simulations sharing the same forcing GCMs; Figure S10). This feature is related to the strong activation of convective rainfall in the MIT-Emanuel convective scheme applied to these simulations as mentioned in previous studies (Juneng *et al.*, 2016; Ngo-Duc *et al.*, 2017; Tangang *et al.*, 2020) The MIT scheme not only produces excessive rainfall (as it is difficult to slow down the convective processes) but it also expands the regions where convective processes occur (Davis *et al.*, 2009). This also helps to explain the widespread amplification of the proportion of convective precipitation over land in RegCM4-3 (all greater than 0.8), which is much higher than in RCA4 and REMO2015 (Figures S12 and S13). It is acknowledged that some of the differences in convective precipitation may be related to the differences in resolution between RCMs and GCMs (Kyselý *et al.*, 2015) even if the convective component is not resolved yet at the resolution of CORDEX-SEA RCMs (i.e., 25 km) but at smaller sub-grid scales (horizontal resolution less than 4 km; Weisman *et al.*, 1997; Prein *et al.*, 2015; Li *et al.*, 2018).

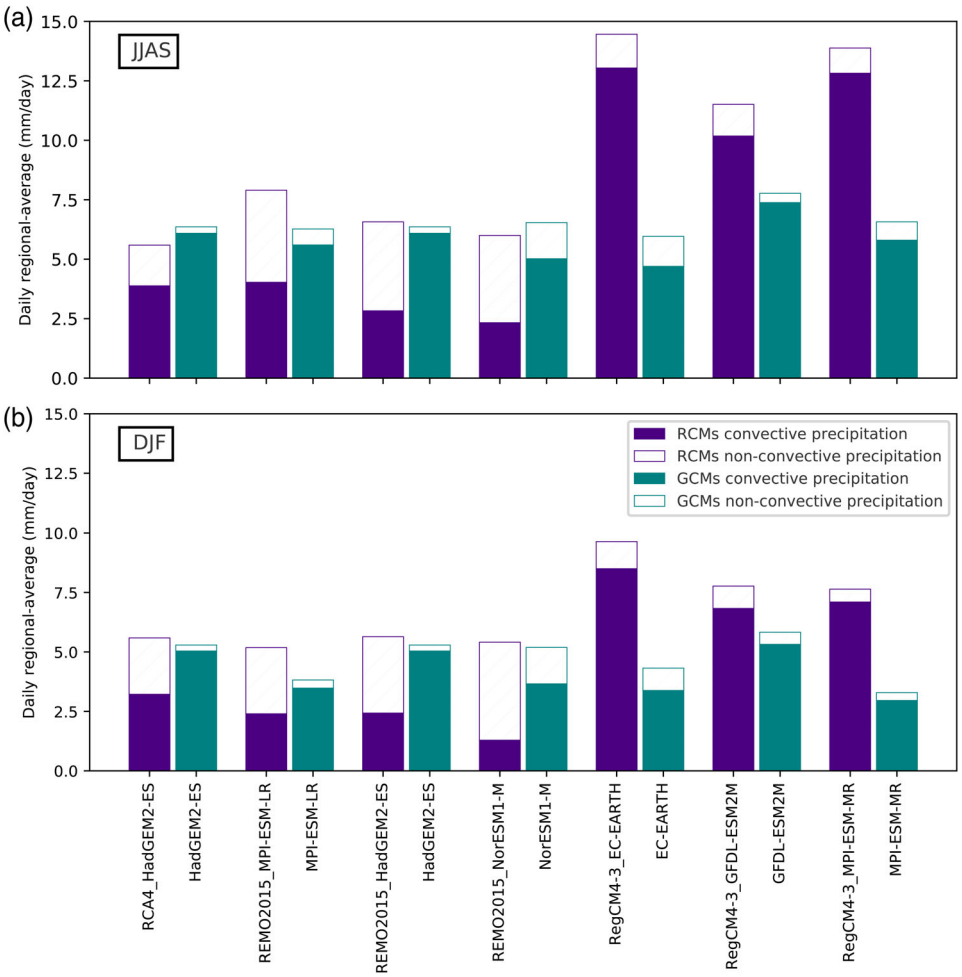

FIGURE 13 Seasonal (JJAS and DJF) mean of daily regional-averaged convective (solid filled) and non-convective (dashed) precipitation (land only; in mm·day^{-1}) simulated by seven available RCMs simulations (Table 1) (purple) and their associated forcing GCMs (green) during the climatological period of 1982–2005

4 | DISCUSSION

The outcome of any model evaluation study is likely dependent on various factors including: the choice of reference dataset(s), the processes and metrics considered, the spatial scale and the domain used. The first major aim of this study is to evaluate the ability of RCMs to simulate both the mean state and distribution of seasonal daily precipitation over SEA in an effort to understand biases in individual models and the MME mean. In general, the performance of individual models in simulating the daily mean state of precipitation is quite similar (i.e., wetter than observed, especially simulations from RegCM4-3), regardless of the choice of observational reference product. The RCM MME mean performs better than any individual ensemble member, consistent with results from Tangang *et al.* (2020). However, the MME mean performance is likely a result of wet and dry biases from individual models cancelling each other out. Interestingly, the ability of a model to simulate the whole distribution of daily precipitation differs substantially among RCMs and is sensitive to the choice of reference product. This is partly explained by the large discrepancies in the precipitation distribution among observations outlined in Section 3.1. In addition, inconsistencies in the frequency of wet days within and between RCMs and observations might somewhat play a role. Among observations, GPCC_v2018 always has the lowest total number of wet days among observations (Figure S14). The RegCM4-3 simulations produce precipitation too frequently while the probability distribution of wet-day frequency among the REMO2015 simulations are quite consistent with observational datasets (Figure S15).

The second aim of the research was to assess differences in each RCM–GCM pairing to capture the precipitation distribution of regionally-averaged daily precipitation. Somewhat surprisingly RCMs were generally "worse" at simulating the distribution of daily precipitation over the region than their forcing GCMs. The results, however, were somewhat dependent on the observational reference product used for evaluation. In particular, most RCMs were closer to GPCC_v2018 (notably during the winter period) compared to their forcing GCMs with respect to the other products considered. GPCC_v2018 has been shown to be wetter in general than other products especially in the upper tails of the distribution but the reason

behind this is still being investigated (Roca *et al.*, 2019; Alexander *et al.*, 2020). While on the surface our results seem somewhat at odds with those of Tangang *et al.* (2020), it highlights those potential biases in individual model simulations could be dampened or exacerbated depending on the observational reference product used for underpinning. Previous studies suggested interpolation to coarser resolution might remove detailed features of RCMs through smoothing the extreme values (Herold *et al.*, 2017), which might affect the scoring metric (ASM) used to measure the proximity between two precipitation distributions in this study. Therefore, we did an additional Q–Q plot for comparison of RCMs, CHIRPSv2 and APHRODITE at ~25 km resolution which is close to both the original resolution of observations and the RCMs resolution (Figures S16 and S17). We find amplified differences between RCMs and observational precipitation distribution even at this higher resolution, which suggests that the coarser resolution of ~240 km used for comparison is not the main reason behind the RCM biases found in this study. This is in line with Bador *et al.* (2020b) who indicate that increasing spatial resolution alone is not sufficient to obtain a systematic improvement in the simulation of precipitation extremes at the global scale.

Our results illustrate that the driving GCMs have less influence on the RCM simulation biases than the choice of RCMs. It is acknowledged that the subset of GCMs that have been downscaled for CORDEX-SEA were chosen for their ability to capture the observed broad-scale characteristics of seasonal monsoonal circulation and precipitation climatology, as is usually done for CORDEX-RCM simulations (Siew *et al.*, 2014; McSweeney *et al.*, 2015). However, most of them show significant biases compared to observed climate patterns. Therefore, another approach of process-based evaluation is generally recommended to assess whether the GCM simulations are capturing the processes (both spatial patterns and magnitude) that drive both mean and extreme precipitation in the region, to fully understand the capability of the GCM. This would help to identify whether there are any GCM–RCM pairings that should not be used at all, in the case where the driving GCMs do not capture the key processes well.

Our results also suggest that the MIT-Emanuel convective scheme is overly active in the RegCM4-3 simulations (at least in the configuration used in these CORDEX-SEA runs) compared to other schemes, resulting in increased precipitation intensity over SEA. In this case 'overactivation' refers to the fact that most of the total precipitation amount in the RCM comes from convective precipitation. This is mostly at odds with what we see in reanalysis products (ERA-interim, ERA5 and MERRA2) over the region (Figures S12j–l and S13j–l) although percentages vary widely (e.g., the ratio of regionally-averaged convective precipitation to total precipitation ranges from 32.97% in MERRA2 to 73.22% in ERA5 during summer; Figures S11 and S12j–l). In all cases the MIT-Emanuel scheme produces a higher proportion of convective precipitation to total precipitation than all other RCM simulations and reanalysis products considered. This is inline with previous regional studies which mentioned the 'overactivation' of the MIT scheme (Juneng *et al.*, 2016; Ngo-Duc *et al.*, 2017). However, the same studies suggested that the MIT scheme performed better than other considered convective schemes, which might somewhat differ from the conclusion we would draw from this study. This can partly be explained by the differences in the experiment setups (set of simulations, reference products and indices). First, the above-mentioned studies evaluate the ERA-interim driven simulations (known as evaluation simulations, which differ from GCM-driven simulations used in this study) against station-based products. This single-point based reference is known to be wetter than grid-based products used in our study, which represents the average precipitation over a particular region. Second, most of their conclusions were also based on frequency-related precipitation indices which differ from the intensity-based and distribution-based metrics used in this study.

Our study provides a simple framework to assess the model performance and takes observational uncertainties into account. Based on the outcome of the model evaluation, it would be interesting to investigate how the selection of particular model ensembles might affect projections under future condition scenarios. Furthermore, our results help to understand the similarities and differences between historical RCMs and their forcing GCMs simulation in the representation of precipitation. Assessing the differences between pairs of RCM and GCM future simulations might be more complex due to the dependency on other external forcings such as greenhouse gases and aerosols. Indeed, it has been shown that the absence of time-varying anthropogenic aerosols in most EURO-CORDEX RCMs tends to lead to a smaller future increase of precipitation over Europe (Boé *et al.*, 2020; Gutiérrez *et al.*, 2020) and such differences in modelling setup might potentially affect the projections over SEA as well.

We have limited our study to SEA, a region which has the advantage of having a large and diverse RCM ensemble. However, this region also has large observational uncertainties (Nguyen *et al.*, 2020), due to a lack of quality high-density station observations. These uncertainties lead to difficulties in evaluating simulated precipitation and therefore our method could benefit from being applied to other Asian regions with higher quality station networks.

5 | CONCLUSION

In this paper, we evaluate the representation of daily precipitation over the 1982–2005 period in high-resolution CORDEX-SEA RCMs over SEA. We focus on two aspects of precipitation: the seasonal mean state and daily precipitation distribution. This study is also the first attempt to assess (a) the performance of individual RCMs relative to their forcing GCMs over SEA and (b) whether or not the driving GCM biases have an influence on the driven RCM biases. Due to the complexities in the spatial distribution of regional climate and its topography, RCMs are usually expected to better represent the daily precipitation distribution (i.e., closer to observed) compared to their forcing GCMs as they are better at resolving sub-grid scales and the processes important for precipitation formation. However, we find that this is often not the case for the CORDEX-SEA simulations evaluated here, despite using four different observational products from different sources (i.e., in situ-based and satellite-based) in order to take the large observational uncertainties in daily precipitation into account. Exploring the physical mechanisms that might play a role in the differences in precipitation between RCMs and GCMs (e.g., contribution of local and large-scale sources of precipitation, role of convective parameterization) are able to understand inter-model differences better.

In general, the CORDEX-SEA RCM simulations show some ability in reproducing the complexities in the spatial distribution of precipitation over the region. However, performance varies substantially across models and also depends on seasons, and evaluation metrics. As noted, this region has large observational uncertainties which leads to difficulties in model evaluations given diverse evaluation metrics and dependence on the choice of reference product. However, despite this, we find that the CORDEX-SEA RCMs generally show a consistently wet bias in seasonal mean precipitation relative to observations, no matter the choice of observational reference product. In addition, considering two skill metrics, some models always perform 'better' (i.e., RCA4_CNRM-CM5) or 'worse' (i.e., REMO2015_HadGEM2-ES and RegCM4-3_EC-EARTH) than other simulations. This will be informative for users in selecting the model that is fit for their purposes.

Because RCMs resolve smaller scales and potentially better represent grid-scale physical processes, they are expected to bring some potential improvements in precipitation simulation compared to their forcing GCMs over the region. Surprisingly, we find that the relative performance of RCMs compared to their GCM depends on the choice of observations. In particular, with three observational products out of four, RCMs do not show reduction in biases. On the whole, the RCMs have a rainfall distribution that is further from observations than the distribution from their driving GCMs. Hence, we cannot find a systematic improvement in the representation of simulated precipitation in RCMs, although there are some parts of the precipitation distribution, seasons and grid points for which RCMs are closer to observations than GCMs. Setting aside observations, RCM simulations are 'wetter' than their counterpart GCM over the region. Further analyses highlight that this wetter state in RCMs is essentially due to the individual RCM setups and not caused by biases or resolution in their forcing GCMs.

This study finds that RCMs generally simulate more intense precipitation over land than their forcing GCMs due to increased local (i.e., evaporation) and large-scale (i.e., moisture convergence) sources of moisture. The question on where this moisture comes from in the RCMs remains to be understood. We also argue that over the region, convective precipitation is generally the largest contributor to total precipitation and leads to the biggest differences in the simulations between the RCMs and GCMs.

Our modelling framework allows us to further investigate inter-model differences by comparing simulated precipitation across RCM simulations forced by the same driving GCM. Substantial differences in the different precipitation quantiles are found and in particular RegCM4-3 systematically produces a wetter bias compared to observations than any other RCM analysed here. This is likely primarily due to the MIT-Emanuel convective scheme adopted in RegCM4, suggesting the important role of parameterization schemes in the resultant quality of RCM simulations. This exploration will be of great interest to RCMs developers or to those involved in using climate model projections to inform the decision making and adaptation (e.g., policymakers). Our study also highlights that great care should be given to the characterization and understanding of the potential discrepancies between RCMs and GCMs and that this could have substantial implications for the interpretation of future precipitation projections over SEA.

AUTHOR CONTRIBUTIONS

Phuong-Loan Nguyen: Formal analysis; methodology; writing – original draft. **Margot Bador:** Methodology; supervision; writing – review and editing. **Lisa V. Alexander:** Supervision; writing – review and editing. **Todd P. Lane:** Supervision; writing – review and editing. **Thanh Ngo-Duc:** Writing – review and editing.

ACKNOWLEDGEMENTS

The authors acknowledge the CORDEX-SEA community for providing the RCM downscaled outputs. All analyses and graphics have been performed using Climate Data Operators (CDO) and Python. Phuong-Loan Nguyen, Lisa V. Alexander and Margot Bador are supported by the

Australian Research Council grant DP160103439. Phuong-Loan Nguyen, Lisa V. Alexander, Margot Bador and Todd P. Lane are supported by the ARC grant CE170100023. Lisa V. Alexander is also supported by ARC grant FT210100459. Thanh Ngo-Duc is supported by the LOTUS International Joint Laboratory. Open access publishing facilitated by University of New South Wales, as part of the Wiley - University of New South Wales agreement via the Council of Australian University Librarians. [Correction added on 19 May 2022, after first online publication: CAUL funding statement has been added.]

CONFLICTS OF INTEREST

The authors declare no conflicts of interest.

ORCID

Phuong-Loan Nguyen https://orcid.org/0000-0003-1041-3514
Margot Bador https://orcid.org/0000-0003-3976-6946

REFERENCES

Alexander, L.V., Bador, M., Roca, R., Contractor, S., Donat, M.G. and Nguyen, P.L. (2020) Intercomparison of annual precipitation indices and extremes over global land areas from in situ, space-based and reanalysis products. *Environmental Research Letters*, 15, 055002. https://doi.org/10.1088/1748-9326/ab79e2.

Bador, M., Alexander, L., Contractor, S. and Roca, R. (2020a) Diverse estimates of annual maxima daily precipitation in 22 state-of-the-art quasi-global land observation datasets. *Environmental Research Letters*, 15, 035005. https://doi.org/10.1088/1748-9326/ab6a22.

Bador, M., Boé, J., Terray, L., Alexander, L., Baker, A., Bellucci, A., Haarsma, R., Koenigk, T., Moine, M.P., Lohmann, K., Putrasahan, D., Roberts, C., Roberts, M., Scoccimarro, E., Schiemann, R., Seddon, J., Senan, R., Valcke, S. and Vannière, B. (2020b) Impact of higher spatial atmospheric resolution on precipitation extremes over land in global climate models. *Journal of Geophysical Research: Atmospheres*, 125, e2019JD032184. https://doi.org/10.1029/2019JD032184.

Boé, J., Somot, S., Corre, L. and Nabat, P. (2020) Large discrepancies in summer climate change over Europe as projected by global and regional climate models: causes and consequences. *Climate Dynamics*, 54, 2981–3002. https://doi.org/10.1007/s00382-020-05153-1.

Brubaker, K.L., Entekhabi, D. and Eagleson, P.S. (1993) Estimation of continental precipitation recycling. *Journal of Climate*, 6, 1077–1089. https://doi.org/10.1175/1520-0442(1993)006<1077:EOCPR>2.0.CO;2.

Chang, C.P., Wang, Z., Mcbride, J. and Liu, C.-H. (2005) Annual cycle of Southeast Asia—Maritime Continent rainfall and the asymmetric monsoon transition. *Journal of Climate*, 18, 287–301. https://doi.org/10.1175/JCLI-3257.1.

Chen, A., Giese, M. and Chen, D. (2020) Flood impact on mainland Southeast Asia between 1985 and 2018—the role of tropical cyclones. *Journal of Flood Risk Management*, 13, e12598. https://doi.org/10.1111/jfr3.12598.

Colin, J., Déqué, M., Radu, R. and Somot, S. (2010) Sensitivity study of heavy precipitation in limited area model climate simulations: influence of the size of the domain and the use of the spectral nudging technique. *Tellus A*, 62, 591–604. https://doi.org/10.1111/j.1600-0870.2010.00467.x.

Contractor, S., Donat, M.G., Alexander, L.V., Ziese, M., Meyer-Christoffer, A., Schneider, U., Rustemeier, E., Becker, A., Durre, I. and Vose, R.S. (2020) Rainfall Estimates on a Gridded Network (REGEN)—a global land-based gridded dataset of daily precipitation from 1950 to 2016. *Hydrology and Earth System Sciences*, 24, 919–943. https://doi.org/10.5194/hess-24-919-2020.

Cruz, F.T., Narisma, G.T., Dado, J.B., Singhruck, P., Tangang, F., Linarka, U.A., Wati, T., Juneng, L., Phan-Van, T., Ngo-Duc, T., Santisirisomboon, J., Gunawan, D. and Aldrian, E. (2017) Sensitivity of temperature to physical parameterization schemes of RegCM4 over the CORDEX-Southeast Asia region. *International Journal of Climatology*, 37, 5139–5153. https://doi.org/10.1002/joc.5151.

Davis, N., Bowden, J., Semazzi, F., Xie, L. and Önol, B. (2009) Customization of RegCM3 regional climate model for eastern Africa and a tropical Indian Ocean domain. *Journal of Climate*, 22, 3595–3616. https://doi.org/10.1175/2009JCLI2388.1.

Demory, M.E., Berthou, S., Fernández, J., Sørland, S.L., Brogli, R., Roberts, M.J., Beyerle, U., Seddon, J., Haarsma, R., Schär, C., Buonomo, E., Christensen, O.B., Ciarlo, J.M., Fealy, R., Nikulin, G., Peano, D., Putrasahan, D., Roberts, C.D., Senan, R., Steger, C., Teichmann, C. and Vautard, R. (2020) European daily precipitation according to EURO-CORDEX regional climate models (RCMs) and high-resolution global climate models (GCMs) from the High-Resolution Model Intercomparison Project (HighResMIP). *Geoscientific Model Development*, 13, 5485–5506. https://doi.org/10.5194/gmd-13-5485-2020.

Demory, M.-E., Vidale, P.L., Roberts, M.J., Berrisford, P., Strachan, J., Schiemann, R. and Mizielinski, M.S. (2014) The role of horizontal resolution in simulating drivers of the global hydrological cycle. *Climate Dynamics*, 42, 2201–2225. https://doi.org/10.1007/s00382-013-1924-4.

Denis, B., Laprise, R., Caya, D. and Côté, J. (2002) Downscaling ability of one-way nested regional climate models: the big-brother experiment. *Climate Dynamics*, 18, 627–646. https://doi.org/10.1007/s00382-001-0201-0.

Di Luca, A., De Elía, R. and Laprise, R. (2012) Potential for added value in precipitation simulated by high-resolution nested regional climate models and observations. *Climate Dynamics*, 38, 1229–1247. https://doi.org/10.1007/s00382-011-1068-3.

Di Virgilio, G., Evans, J.P., Di Luca, A., Grose, M.R., Round, V. and Thatcher, M. (2020) Realised added value in dynamical downscaling of Australian climate change. *Climate Dynamics*, 54, 4675–4692. https://doi.org/10.1007/s00382-020-05250-1.

Diaconescu, E.P. and Laprise, R. (2013) Can added value be expected in RCM-simulated large scales? *Climate Dynamics*, 41, 1769–1800. https://doi.org/10.1007/s00382-012-1649-9.

Dickinson, R.E., Henderson-Sellers, A., Kennedy, P.J. & Wilson, M. F. (1986) *Biosphere-Atmosphere Transfer Scheme (BATS) for the NCAR Community Climate Model*. University Corporation for Atmospheric Research. NCAR/TN-275+STR.

Donat, M.G., Alexander, L.V., Herold, N. and Dittus, A.J. (2016) Temperature and precipitation extremes in century-long gridded observations, Reanalyses, and atmospheric model simulations. *Journal of Geophysical Research: Atmospheres*, 121, 11174–11189. https://doi.org/10.1002/2016JD025480.

Emanuel, K. and Rothman, M. (1999) Development and evaluation of a convection scheme for use in climate models. *Journal of the Atmospheric Sciences*, 56, 1766–1782. https://doi.org/10.1175/1520-0469(1999)056<1766:DAEOAC>2.0.CO;2.

Endo, H. and Kitoh, A. (2014) Thermodynamic and dynamic effects on regional monsoon rainfall changes in a warmer climate. *Geophysical Research Letters*, 41, 1704–1711. https://doi.org/10.1002/2013GL059158.

Fritsch, J.M. and Kain, J.S. (1993) Convective parameterization for mesoscale models: the Fritsch-Chappell scheme. In: Emanuel, K.A. and Raymond, D.J. (Eds.) *The Representation of Cumulus Convection in Numerical Models*. Boston, MA: American Meteorological Society, pp. 165–170. https://doi.org/10.1007/978-1-935704-13-3_15.

Funk, C., Peterson, P., Landsfeld, M., Pedreros, D., Verdin, J., Shukla, S., Husak, G., Rowland, J., Harrison, L., Hoell, A. and Michaelsen, J. (2015) The climate hazards Infrared precipitation with stations—a new environmental record for monitoring extremes. *Scientific Data*, 2, 150066. https://doi.org/10.1038/sdata.2015.66.

Giorgi, F. and Bates, G. (1989) The climatological skill of a regional model over complex terrain. *Monthly Weather Review*, 117, 2325–2347. https://doi.org/10.1175/1520-0493(1989)117<2325:TCSOAR>2.0.CO;2.

Giorgi, F. and Gutowski, W.J. (2016) Coordinated experiments for projections of regional climate change. *Current Climate Change Reports*, 2, 202–210. https://doi.org/10.1007/s40641-016-0046-6.

Giorgi, F. and Gutowski, W.J., Jr. (2015) Regional dynamical downscaling and the CORDEX initiative. *Annual Review of Environment and Resources*, 40, 467–490. https://doi.org/10.1146/annurev-environ-102014-021217.

Giorgi, F., Jones, C. and Asrar, G. (2008) Addressing climate information needs at the regional level: the CORDEX framework. *WMO Bulletin*, 53, 175.

Goergen, K. and Kollet, S. (2021) Boundary condition and oceanic impacts on the atmospheric water balance in limited area climate model ensembles. *Scientific Reports*, 11, 6228. https://doi.org/10.1038/s41598-021-85744-y.

Gutiérrez, C., Somot, S., Nabat, P., Mallet, M., Corre, L., Meijgaard, E., Perpiñán, O. and Gaertner, M. (2020) Future evolution of surface solar radiation and photovoltaic potential in Europe: investigating the role of aerosols. *Environmental Research Letters*, 15, 034035. https://doi.org/10.1088/1748-9326/ab6666.

Hagemann, S. (2002) *An improved land surface parameter dataset for global and regional climate models*. Max-Planck-Institut für Meteorologie. Technical Report 336. https://doi.org/10.17617/2.2344576

Herold, N., Alexander, L.V., Donat, M.G., Contractor, S. and Becker, A. (2016) How much does it rain over land? *Geophysical Research Letters*, 43, 341–348. https://doi.org/10.1002/2015GL066615.

Herold, N., Behrangi, A. and Alexander, L.V. (2017) Large uncertainties in observed daily precipitation extremes over land. *Journal of Geophysical Research: Atmospheres*, 122, 668–681. https://doi.org/10.1002/2016JD025842.

Hijioka, Y., Lin, E., Pereira, J.J., Corlett, R.T., Cui, X., Insarov, G.E., Lasco, R.D., Lindgren, E. and Surjan, A. (2014) *Asia. Climate Change 2014: Impacts, Adaptation, and Vulnerability. Part B: Regional Aspects. Contribution of Working Group Ii to the Fifth Assessment Report of the Intergovernmental Panel on Climate Change*. Cambridge, United Kingdom and New York, NY, USA: Cambridge University Press.

IPCC. (2013) *Climate change 2013: the physical science basis: Contribution of Working Group I to the Fifth Assessment Report of the Intergovernmental Panel on Climate Change*. Cambridge, United Kingdom and New York, NY, USA: Cambridge University Press. https://doi.org/10.1017/CBO9781107415324.

Juneng, L., Tangang, F., Chung, J.X., Ngai, S.T., Teh, T.W., Narisma, G., Cruz, F., Phan-Van, T., Ngo-Duc, T., Santisirisomboon, J., Singhruck, P., Gunawan, D. and Aldrian, E. (2016) Sensitivity of Southeast Asia rainfall simulations to cumulus and Air–Sea flux parameterizations in RegCM4. *Climate Research*, 69, 59–77. https://doi.org/10.3354/cr01386.

Kamworapan, S. and Surussavadee, C. (2019) Evaluation of CMIP5 global climate models for simulating climatological temperature and precipitation for Southeast Asia. *Advances in Meteorology*, 2019, 1067365. https://doi.org/10.1155/2019/1067365.

Kotlarski, S., Keuler, K., Christensen, O.B., Colette, A., Déqué, M., Gobiet, A., Goergen, K., Jacob, D., Lüthi, D., Van Meijgaard, E., Nikulin, G., Schär, C., Teichmann, C., Vautard, R., Warrach-Sagi, K. and Wulfmeyer, V. (2014) Regional climate modeling on European scales: a joint standard evaluation of the EURO-CORDEX RCM ensemble. *Geoscientific Model Development*, 7, 1297–1333. https://doi.org/10.5194/gmd-7-1297-2014.

Kotlarski, S., Szabó, P., Herrera, S., Räty, O., Keuler, K., Soares, P. M., Cardoso, R.M., Bosshard, T., Pagé, C., Boberg, F., Gutiérrez, J.M., Isotta, F.A., Jaczewski, A., Kreienkamp, F., Liniger, M.A., Lussana, C. and Pianko-Kluczyńska, K. (2019) Observational uncertainty and regional climate model evaluation: a pan-European perspective. *International Journal of Climatology*, 39, 3730–3749. https://doi.org/10.1002/joc.5249.

Kyselý, J., Rulfova, Z., Farda, A. and Hanel, M. (2015) Convective and stratiform precipitation characteristics in an ensemble of regional climate model simulations. *Climate Dynamics*, 46, 227–243. https://doi.org/10.1007/s00382-015-2580-7.

Lee, D., Min, S.-K., Jin, J., Lee, J., Cha, D.-H., Suh, M.-S., Ahn, J.B., Hong, S.-Y., Kang, H.-S. and Joh, M. (2017) Thermodynamic and dynamic contributions to future changes in summer precipitation over Northeast Asia and Korea: a multi-RCM study. *Climate Dynamics*, 49, 4121–4139. https://doi.org/10.1007/s00382-017-3566-4.

Li, L., Li, W. and Barros, A.P. (2013) Atmospheric moisture budget and its regulation of the summer precipitation variability over the southeastern United States. *Climate Dynamics*, 41, 613–631. https://doi.org/10.1007/s00382-013-1697-9.

Li, J., Wasko, C., Johnson, F., Evans, J.P. and Sharma, A. (2018) Can regional climate modeling capture the observed changes in spatial Organization of Extreme Storms at higher temperatures? *Geophysical Research Letters*, 45, 4475–4484. https://doi.org/10.1029/2018GL077716.

McSweeney, C.F., Jones, R.G., Lee, R.W. and Rowell, D.P. (2015) Selecting CMIP5 GCMs for downscaling over multiple regions. *Climate Dynamics*, 44, 3237–3260. https://doi.org/10.1007/s00382-014-2418-8.

Meehl, G., Boer, G., Covey, C., Latif, M. and Ronald, S. (2000) CMIP Coupled Model Intercomparison Project. *Bulletin of the American Meteorological Society*, 81, 313–318. https://doi.org/10.1175/1520-0477(2000)081<0313:TCMIPC>2.3.CO;2.

Ngo-Duc, T., Tangang, F.T., Santisirisomboon, J., Cruz, F., Trinh-Tuan, L., Nguyen-Xuan, T., Phan-Van, T., Juneng, L., Narisma, G., Singhruck, P., Gunawan, D. and Aldrian, E. (2017) Performance evaluation of RegCM4 in simulating extreme rainfall and temperature indices over the CORDEX-Southeast Asia region. *International Journal of Climatology*, 37, 1634–1647. https://doi.org/10.1002/joc.4803.

Nguyen, P.-L., Bador, M., Alexander, L.V., Lane, T.P. and Funk, C. C. (2020) On the robustness of annual daily precipitation maxima estimates over monsoon Asia. *Frontiers in Climate*, 2, 578785. https://doi.org/10.3389/fclim.2020.578785.

Nguyen-Thi, T., Ngo-Duc, T., Tangang, F.T., Cruz, F., Juneng, L., Santisirisomboon, J., Aldrian, E., Phan-Van, T. and Narisma, G. (2021) Climate analogue and future appearance of novel climate in Southeast Asia. *International Journal of Climatology*, 41, E392–E409. https://doi.org/10.1002/joc.6693.

Nikulin, G., Jones, C., Giorgi, F., Asrar, G., Büchner, M., Cerezo-Mota, R., Christensen, O., Dqu, M., Fernández, J., Haensler, A., Meijgaard, E., Samuelsson, P., Sylla, M. and Sushama, L. (2012) Precipitation climatology in an ensemble of CORDEX-Africa regional climate simulations. *Journal of Climate*, 25, 6057–6078. https://doi.org/10.1175/JCLI-D-11-00375.1.

Park, C., Cha, D.-H., Kim, G., Lee, G., Lee, D.-K., Suh, M.-S., Hong, S.-Y., Ahn, J.B. and Min, S.-K. (2019) Evaluation of summer precipitation over Far East Asia and South Korea simulated by multiple regional climate models. *International Journal of Climatology*, 40, 2270–2284. https://doi.org/10.1002/joc.6331.

Prein, A.F., Bukovsky, M.S., Mearns, L.O., Bruyère, C.L. and Done, J.M. (2019) Simulating North American weather types with regional climate models. *Frontiers in Environmental Science*, 7, 36. https://doi.org/10.3389/fenvs.2019.00036.

Prein, A.F., Gobiet, A., Truhetz, H., Keuler, K., Goergen, K., Teichmann, C., Fox Maule, C., Van Meijgaard, E., Déqué, M., Nikulin, G., Vautard, R., Colette, A., Kjellström, E. and Jacob, D. (2016) Precipitation in the EURO-CORDEX 0.11° and 0.44° simulations: high resolution, high benefits? *Climate Dynamics*, 46, 383–412. https://doi.org/10.1007/s00382-015-2589-y.

Prein, A.F., Langhans, W., Fosser, G., Ferrone, A., Ban, N., Goergen, K., Keller, M., Tölle, M., Gutjahr, O., Feser, F., Brisson, E., Kollet, S., Schmidli, J., Van Lipzig, N.P.M. and Leung, R. (2015) A review on regional convection-permitting climate modeling: demonstrations, prospects, and challenges. *Reviews of Geophysics*, 53, 323–361. https://doi.org/10.1002/2014RG000475.

Rechid, D., Hagemann, S. and Jacob, D. (2009) Sensitivity of climate models to seasonal variability of snow-free land surface albedo. *Theoretical and Applied Climatology*, 95, 197–221. https://doi.org/10.1007/s00704-007-0371-8.

Robertson, A., Moron, V., Qian, J., Chang, C.-P., Tangang, F., Aldrian, E., Koh, T. and Juneng, L. (2011) The maritime continent monsoon. In: Chang, C.-P., Ding, Y., Lau, N.-C., Johnson, R.H., Wang, B. and Yasunari, T. (Eds.) *The Global Monsoon System*. Singapore: World Scientific Publishing Company, pp. 85–98. https://doi.org/10.1142/9789814343411_0006.

Roca, R., Alexander, L.V., Potter, G., Bador, M., Jucá, R., Contractor, S., Bosilovich, M.G. and Cloché, S. (2019) Frogs: a daily 1° × 1° gridded precipitation database of rain gauge, satellite and reanalysis products. *Earth System Science Data*, 11, 1017–1035. https://doi.org/10.5194/essd-11-1017-2019.

Samuelsson, P., Gollvik, S. and Ullerstig, A. (2006) *The Land-Surface Scheme of the Rossby Centre Regional Atmospheric Climate Model (RCA3)*. Sweden: SMHI.

Schamm, K., Ziese, M., Becker, A., Finger, P., Meyer-Christoffer, A., Schneider, U., Schröder, M. and Stender, P. (2014) Global gridded precipitation over land: a description of the new GPCC first guess daily product. *Earth System Science Data*, 6, 49–60. https://doi.org/10.5194/essd-6-49-2014.

Seager, R. and Henderson, N. (2013) Diagnostic computation of moisture budgets in the ERA-interim reanalysis with reference to analysis of CMIP-archived atmospheric model data. *Journal of Climate*, 26, 7876–7901. https://doi.org/10.1175/JCLI-D-13-00018.1.

Seager, R., Henderson, N. and Vecchi, G. (2010) Thermodynamic and dynamic mechanisms for large-scale changes in the hydrological cycle in response to global warming. *Journal of Climate*, 23, 4651–4668. https://doi.org/10.1175/2010JCLI3655.1.

Sein, D.V., Mikolajewicz, U., Gröger, M., Fast, I., Cabos, W., Pinto, J.G., Hagemann, S., Semmler, T., Izquierdo, A. and Jacob, D. (2015) Regionally coupled atmosphere-ocean-sea ice-marine biogeochemistry model ROM: 1. Description and validation. *Journal of Advances in Modeling Earth Systems*, 7, 268–304. https://doi.org/10.1002/2014MS000357.

Siew, J.H., Tangang, F.T. and Juneng, L. (2014) Evaluation of CMIP5 coupled Atmosphere–Ocean general circulation models and projection of the southeast Asian winter monsoon in the 21st century. *International Journal of Climatology*, 34, 2872–2884. https://doi.org/10.1002/joc.3880.

Solman, S.A. and Blázquez, J. (2019) Multiscale precipitation variability over South America: analysis of the added value of CORDEX RCM simulations. *Climate Dynamics*, 53, 1547–1565. https://doi.org/10.1007/s00382-019-04689-1.

Tangang, F., Chung, J.X., Juneng, L., Supari Salimun, E., Ngai, S.T., Jamaluddin, A.F., Mohd, M.S.F., Cruz, F., Narisma, G., Santisirisomboon, J., Ngo-Duc, T., Van Tan, P., Singhruck, P., Gunawan, D., Aldrian, E., Sopaheluwakan, A., Grigory, N., Remedio, A.R.C., Sein, D.V., Hein-Griggs, D., Mcgregor, J.L., Yang, H., Sasaki, H. and Kumar, P. (2020) Projected future changes in rainfall in Southeast Asia based on CORDEX–SEA multi-model simulations. *Climate Dynamics*, 55, 1247–1267. https://doi.org/10.1007/s00382-020-05322-2.

Tangang, F., Farzanmanesh, R., Mirzaei, A., Supari Salimun, E., Jamaluddin, A.F. and Juneng, L. (2017) Characteristics of precipitation extremes in Malaysia associated with El Niño and La Niña events. *International Journal of Climatology*, 37, 696–716. https://doi.org/10.1002/joc.5032.

Tangang, F., Santisirisomboon, J., Juneng, L., Salimun, E., Chung, J., Supari, S., Cruz, F., Ngai, S.T., Ngo-Duc, T., Singhruck, P., Narisma, G., Santisirisomboon, J.,

Wongsaree, W., Promjirapawat, K., Sukamongkol, Y., Srisawadwong, R., Setsirichok, D., Phan-Van, T., Aldrian, E., Gunawan, D., Nikulin, G. and Yang, H. (2019) Projected future changes in mean precipitation over Thailand based on multi-model regional climate simulations of CORDEX Southeast Asia. *International Journal of Climatology*, 39, 5413–5436. https://doi.org/10.1002/joc.6163.

Tiedtke, M. (1989) A comprehensive mass flux scheme for cumulus parameterization in large-scale models. *Monthly Weather Review*, 117, 1779. https://doi.org/10.1175/1520-0493(1989)117<1779:Acmfsf>2.0.Co;2.

Torma, C., Giorgi, F. and Coppola, E. (2015) Added value of regional climate modeling over areas characterized by complex terrain—precipitation over the Alps. *Journal of Geophysical Research: Atmospheres*, 120, 3957–3972. https://doi.org/10.1002/2014JD022781.

Vannière, B., Demory, M.-E., Vidale, P.L., Schiemann, R., Roberts, M.J., Roberts, C.D., Matsueda, M., Terray, L., Koenigk, T. and Senan, R. (2019) Multi-model evaluation of the sensitivity of the global energy budget and hydrological cycle to resolution. *Climate Dynamics*, 52, 6817–6846. https://doi.org/10.1007/s00382-018-4547-y.

Waliser, D. and Gautier, C. (1993) A satellite-derived climatology of the ITCZ. *Journal of Climate*, 6, 2162–2174. https://doi.org/10.1175/1520-0442(1993)006<2162:ASDCOT>2.0.CO;2.

Weisman, M.L., Skamarock, W.C. and Klemp, J.B. (1997) The resolution dependence of explicitly modeled convective systems. *Monthly Weather Review*, 125, 527–548. https://doi.org/10.1175/1520-0493(1997)125<0527:Trdoem>2.0.Co;2.

Weiss, J. (2009) *The Economics of Climate Change in Southeast Asia: A Regional Review*. Mandaluyong, Philippines: Asian Development Bank. http://hdl.handle.net/11540/179. License: CC BY 3.0 IGO.

Yang, B., Qian, Y., Lin, G., Leung, R. and Zhang, Y. (2012) Some issues in uncertainty quantification and parameter tuning: a case study of convective parameterization scheme in the WRF regional climate model. *Atmospheric Chemistry and Physics*, 12, 2409–2427. https://doi.org/10.5194/acp-12-2409-2012.

Yatagai, A., Yasutomi, N., Hamada, A., Kitoh, A., Kamiguchi, K. and Arakawa, O. (2012) Aphrodite: constructing a long-term daily gridded precipitation dataset for asia based on a dense network of rain gauges. *Bulletin of the American Meteorological Society*, 93, 1401–1415.

SUPPORTING INFORMATION

Additional supporting information may be found in the online version of the article at the publisher's website.

How to cite this article: Nguyen, P.-L., Bador, M., Alexander, L. V., Lane, T. P., & Ngo-Duc, T. (2022). More intense daily precipitation in CORDEX-SEA regional climate models than their forcing global climate models over Southeast Asia. *International Journal of Climatology*, 1–25. https://doi.org/10.1002/joc.7619